JOURNAL OF GEOPHYSICAL RESEARCH, VOL. 100, NO. B2, PAGES 2069–2087, FEBRUARY 10, 1995

Significance of seismic reflections beneath a tilted exposure of deep continental crust, Tehachapi Mountains, California

P. E. Malin,[1,2] E. D. Goodman,[3,4] T. L. Henyey,[5] Y. G. Li,[5] D. A. Okaya,[5] and J. B. Saleeby [6]

Abstract. The focus of this article is a process whereby lower crustal crystalline and schistose rocks can rise to the surface, with the Tehachapi Mountains in California being the case in point. As a prime example of the lower crust, these mountains expose Cretaceous gneisses that formed 25-30 km down in the Sierra Nevada batholith and appear to be underlain by the ensimatic Rand schist. Integrated geophysical and geological studies by the CALCRUST program have produced a cross section through this post-Mid-Cretaceous structure and suggest a general model for its development. Seismic reflection and refraction profiles show that the batholithic rocks dip northward as a tilted slab and extend beneath the southern end of the San Joaquin Basin's Tejon embayment. Two south dipping reverse faults on the rim of the Tejon embayment were discovered in the reflection data and verified in the field. The faults have a combined separation of several kilometers and cut through an upper crustal reflection zone that projects to the surface outcrop of the Rand schist. The upper and lower crusts are separated by a zone of laterally discontinuous reflectors. Reflections from the lower crust form a wedge, the base of which is a nearly flat Moho at 33 km. Regional geological relations and gravity models both suggest that the reflective zone corresponds to the Rand schist and the newly recognized faults account for its Neogene exposure. Alternatively, the reflective zone maybe part of the gneiss complex, suggesting that the schist either lies deeper or is not present under the gneisses. If the Rand schist underlies the Tehachapi Mountains and Mojave region to their south, a model for their evolution can be constructed from regional geological relations. It seems that during Late Cretaceous Laramide subduction the protolith of the schist was thrust eastward beneath the Mojave. Along this portion of the Cordilleran batholithic belt the subduction was evidently at very low angles. The bottom of the batholith was removed and replaced by a thick section of schist, fluids from which weakened the overlying batholith. This thickened crust collapsed by horizontal flow in the schist and faulting of the upper crust into flat-lying slabs. When emplacement of the schist ended in latest Cretaceous/earliest Paleocene, the underlying mantle rose, compensating for the extension and providing material for magmatic underplating. In the Neogene, transpression and rotation of the upper crust along the San Andreas and Garlock faults resulted in the exposure of the schist.

Introduction

The Tehachapi Mountains' gneiss complex dips northwestward under the Cenozoic sediments of the San Joaquin Valley's Tejon embayment, at the southernmost tip of the San Joaquin Basin (SSJB) (Figure 1). The gneisses are bounded on the south by the Garlock fault and an exposure of Rand schist (Figure 2) [*Wiese*, 1950]. Regional geology, petrology, geophysics, and seismology all suggest that the Rand schist represents an ensimatic protolith that was thrust beneath the gneisses during the Late Cretaceous and which may underlie both the Tehachapi Mountains and Tejon embayment, as well as the Mojave Desert to their south (Figure 2) [e.g., *Ehlig*, 1968; *Silver*, 1982, 1983; *Plescia*, 1985; *Cheadle et al.*, 1986; *Carter*, 1987; *Lawson*, 1989]. The processes and resulting crustal structure that bring the gneiss and Rand schist to the surface are the focus of this paper (see also *Salisbury and Fountain* [1990]).

The Tehachapi Mountains' gneisses are thought to represent the Cretaceous mid-to-lower crust of the Sierra Nevada batholith [*Saleeby et al.*, 1987; *Saleeby*, 1990; *Pickett and Saleeby*, 1993]. Both the gneisses and the presumably underlying schist were uplifted in the latest Cretaceous/early Paleocene and exposed in the Tertiary [*Jacobson et al.*, 1988; *Goodman*, 1989; *Silver and Nourse*, 1986; *Pickett and Saleeby*, 1993]. The uplifted Tehachapi block apparently experienced Neogene clockwise rotation and late Miocene-to-Recent thrusting along the White Wolf fault (WWF), placing these basement rocks over the 12-km-deep SSJB [e.g., *McWilliams and Li*, 1985; *Goodman and Malin*, 1992].

The Tehachapi Mountains study described here was part of the California Consortium for Crustal Studies (CALCRUST) effort to understand the relationships between surface exposures of high-grade Mesozoic metamorphic rocks, associated faults, and lower crustal processes [e.g., *Henyey et al.*, 1987]. In the Tehachapi Mountains, CALCRUST acquired a 38-km reflection profile and

[1]Department of Geology, Duke University, Durham, North Carolina.

[2]Formerly Institute for Crustal Studies University of California, Santa Barbara.

[3]Institute for Crustal Studies University of California, Santa Barbara.

[4]Now at Exxon Production Research Company, Houston, Texas.

[5]Department of Geological Sciences, University of Southern California, Los Angeles.

[6]Division of Geological and Planetary Sciences, California Institute of Technology, Pasadena.

Paper number 94JB02127.
0148-0227/95/94JB-02127$05.00

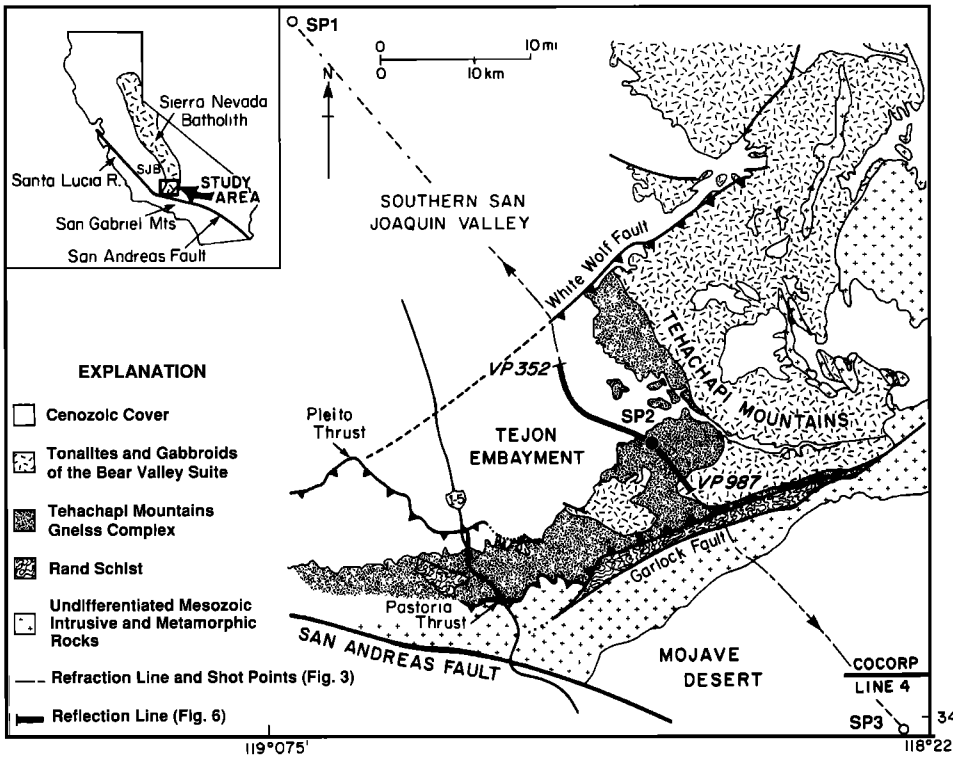

Figure 1. Index and location maps for the Tehachapi Mountains-Tejon embayment area in south-central California's San Joaquin Basin. Also shown is that portion of the CALCRUST seismic reflection profile containing deep reflections and discussed in this paper (between vibration points VP 352 to VP 987). Important geological features are the exposed Mesozoic basement rocks; their Cenozoic sedimentary cover in the Tejon embayment (modified from *Sams and Saleeby* [1988]); and the Rand schist outcrop and Rand thrust/north branch of the Garlock fault on its north side [e.g., *Buwalda,* 1954; *Burchfiel and Davis*, 1981]. Other seismic survey lines are the overlying CALCRUST refraction profile [from *Goodman et al.,* 1989] and the most northwestern line of the COCORP Mojave Desert reflection survey, line 4 [from *Cheadle et al.*, 1986].

a coincident 110-km refraction profile [*Malin et al.*, 1988; *Ambos and Malin,* 1987]. Further constraints were obtained from newly compiled gravity data (J. Plescia, Jet Propulsion Laboratory, Pasadena, California, unpublished data, 1993) and industry reflection and well log measurements in the Tejon embayment [*Goodman and Malin*, 1988; *Goodman et al.,* 1989; *Goodman*, 1989; *Goodman and Malin*, 1992]. The CALCRUST reflection profile was begun a few kilometers north of the WWF. From there it was taken south, toward line 4 of the Consortium for Continental Reflection Profiling (COCORP) Mojave Desert survey (Figure 2) [*Cheadle et al.,* 1986], until the project budget was exhausted about a kilometer north of the Rand schist outcrop. A central, 22-km-long segment of the CALCRUST data contains clear deep reflections (Figures 1 and 2). This segment is entirely south of the WWF, whose multiple strands and complex folding produce a bad data area for deeper signals [e.g., *Goodman and Malin*, 1992]. The segment also lies 4 km north of the Rand schist, the southern 3 km of data being eliminated because of severe signal-generated noise, out-of-plane reflections, and reflected refractions.

The refraction data, which penetrated to midcrustal levels (<15 km), show several significant features. They include (1) velocity discontinuities in the areas of the Garlock fault and WWF, (2) high-velocity rock units at shallow depths beneath the site of the reflection survey, and (3) a northwest dip in these units (Figure 3c) [*Goodman et al.,* 1989]. Because of the effects of averaging, the refraction models cannot resolve the locations and amounts of dip in laterally varying structures. Thus the gravity and reflection data add essential constraints to the refraction model (Figures 3, 5, 6, and 7). As in the general cases discussed by *Barton* [1986], a relatively broad range of velocity-density relations was required to obtain a consistent model for both the seismic and gravity data from the Tehachapi Mountains.

The CALCRUST reflection profile aimed principally at addressing the structural relationship of the gneiss and schist, their distribution in the crust, and the response of the crust to latest Mesozoic and Cenozoic tectonics. The depth-converted common midpoint (CMP) stack of these data shows (1) a series of northwest dipping reflections consistent with the refraction results, (2) a midcrustal change in reflection character, (3) a wedge of reflectors in the lower crust with variable northwesterly dips and hinge points at or near the Moho, and (4) a relatively flat, 33-km-deep Moho. A similar Moho structure was previously found in the earthquake tomography of *Hearn and Clayton* [1986a, b] and simple gravity model of *Plescia* [1985]. The gravity model suggests that the topography of the Tehachapi Mountains may be supported at relatively shallow levels, perhaps even within the crust. This might be the case, for example, if the Tehachapi gneiss complex is underlain by a body of slightly faster but slightly less dense schist.

In total, the geology and geophysics of the crust beneath the Tejon embayment and Tehachapi Mountains suggest an event of

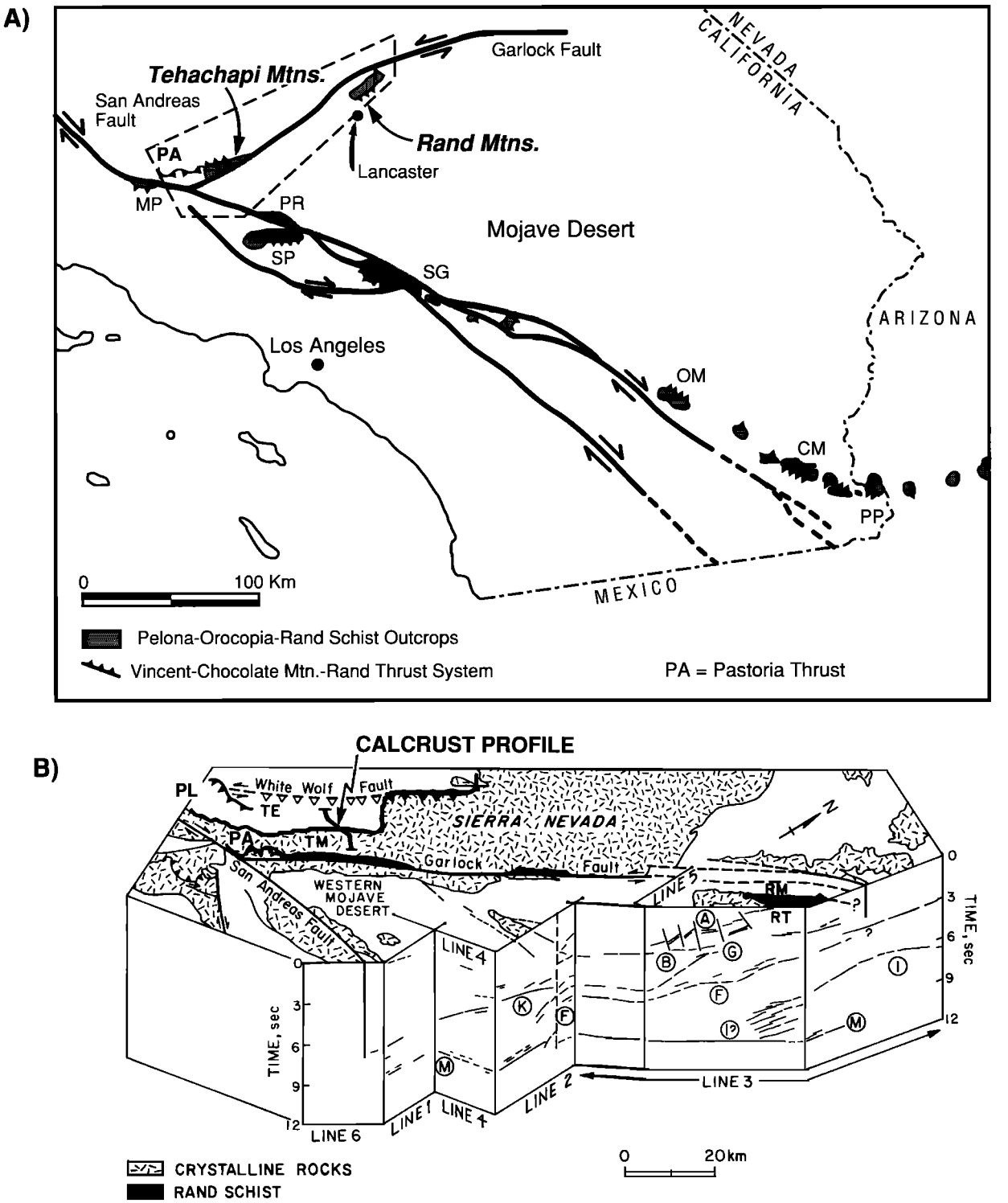

Figure 2. (a) Map showing major active structural features and present-day exposures of Pelona-Orocopia-Rand schists. The Vincent-Chocolate-Rand thrust system, indicated by teeth on the schist bodies, is of Mesozoic age. Using U.S. Geological Survey, COCORP, and industry seismic data, *Lawson* [1989], for example, has argued that schist underlies a large part of the western Mojave Desert. Besides those in the Tehachapi and Rand Mountains, the various schist outcrops denoted are Mount Pinos (MP), Portal and Ritter ridges (PR), Sierra Pelona (SP), San Gabriel Mountains (SG), Orocopia Mountains (OM), Chocolate Mountains (CM), and Picacho Peak (PP) area (modified from *Jacobson* [1983]); (b) Block diagram and line drawings of the reflection structure of the western Mojave Desert from the COCORP Mojave Desert reflection profiles. The approximate map location of this diagram is indicated by the dashed polygon in Figure 2a. Also shown are the locations of the CALCRUST Tehachapi Mountains profile, the Tehachapi Mountains (TM), the Tejon embayment (TE), the Pastoria thrust (PA), the Pleito thrust (PL), the Rand Mountains (RM), and the Rand thrust (RT) in the Rand Mountains. The Mojave Desert reflection lines and their reflection horizons are shown in a cutaway section along profile [after *Cheadle et al.*, 1986]. The Rand schist may project under much of the western Mojave Desert. Note the high-angle structures interpreted as cutting through reflection horizon A, the reflector interpreted as the Rand thrust at the top of the Rand schist.

upward tilt to the southeast by as much as 25°. This process took place between mid-Cretaceous and early Paleogene in association with the emplacement and uplift of the Rand schist [*Jacobson*, 1990; *Pickett and Saleeby*, 1993]. The seismic data confirm borehole evidence that deep Sierran crystalline rocks extend beneath the Tejon embayment. At somewhat greater depths, the reflection data suggest that the Rand schist underlies the central profile segment. With the possible exception of requiring schist velocities several percent higher than those observed by *Malin et al.* [1981], this interpretation is consistent, within errors, with the refraction and gravity data. The tilted upper crust also steps upward to the south across two previously unrecognized, high-angle, southeast dipping faults of late Neogene age. In the present, transpression along the Garlock fault and WWF zones

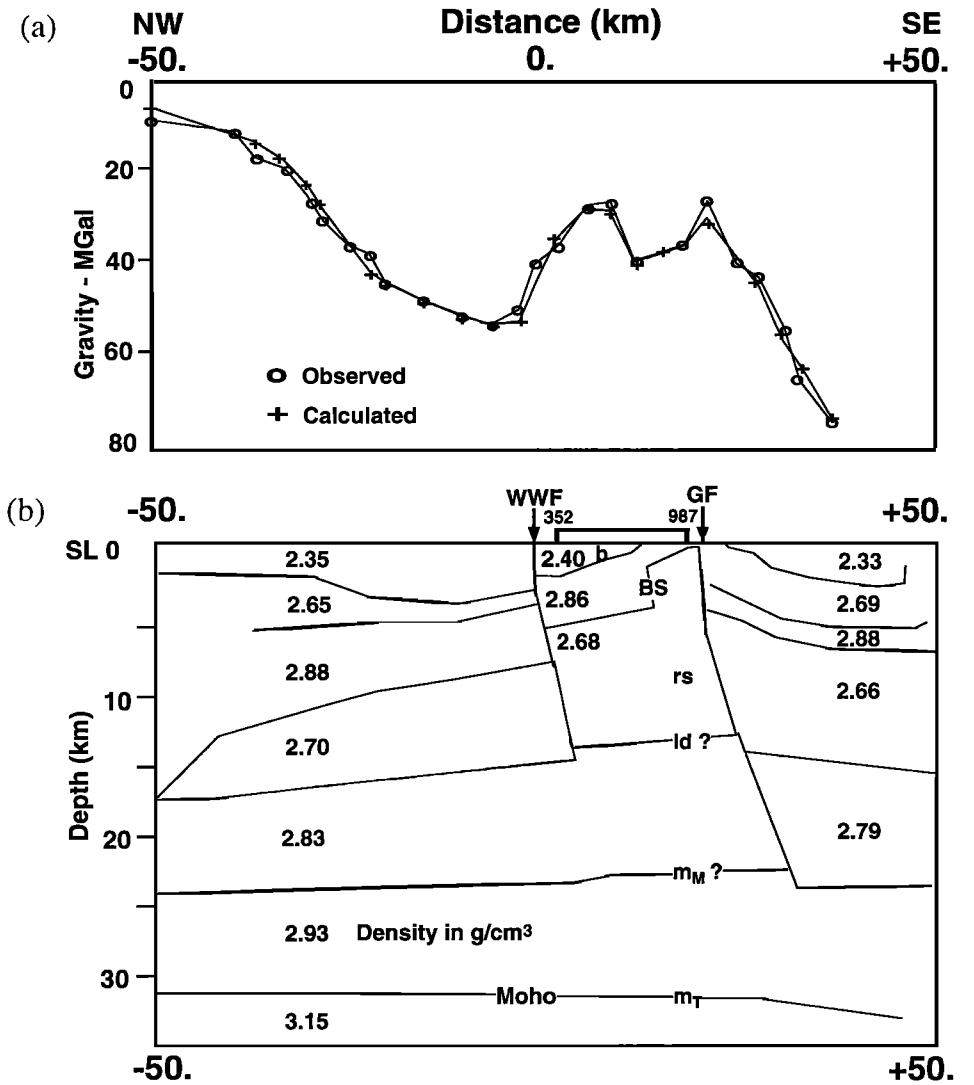

Figure 3. Forward crustal models of the gravity field and velocity structure over the CALCRUST Tehachapi Mountains survey profile. (a) The gravity data and (b) gravity model are modified from *Plescia* [1985] and J.B. Plescia (unpublished data and forward models, 1992). The gravity modeling followed the methods of *Barton* [1986]. (c) The *P* wave velocity structure is from forward modeling of the CALCRUST Tehachapi Mountains refraction survey shown in Figure 1. This model is a modified version of the one proposed by *Ambos and Malin* [1987] and *Goodman et al.* [1989]. The surface positions of the refraction shot points are indicated by arrows, as are the White Wolf (WWF) and Garlock (GF) faults, which are depicted as south dipping features. In the uppermost crust, where resolutions of the gravity and refraction data are poor, the structure was taken from the reflection data. Depths are in kilometers, densities are shown in grams per cubic centimeter, and velocities in kilometers per second, with their range given by the values at the top and bottom of the layers. The most significant feature of the gravity fit is the slightly lower density body below the gneisses of the Tehachapi block. Our estimates of the error (1 standard deviation) in depth, density, and velocity are 1 km, 0.1 g/cm^3, and 0.15 km/s, respectively. Note that the thickness of the crust is nearly constant in these simple models. In fact, at a depth of 32 km, the masses of the various crustal columns along this profile differ by less than these uncertainties. Dashed boundaries in the velocity model indicate the areas where these limit are likely to be exceeded. The annotated zones are interpreted as basin and basin bottom (b), Rand schist (rs), crustal scale decollement or brittle/ductile transition zone (ld), and Beno Springs fault (BS).

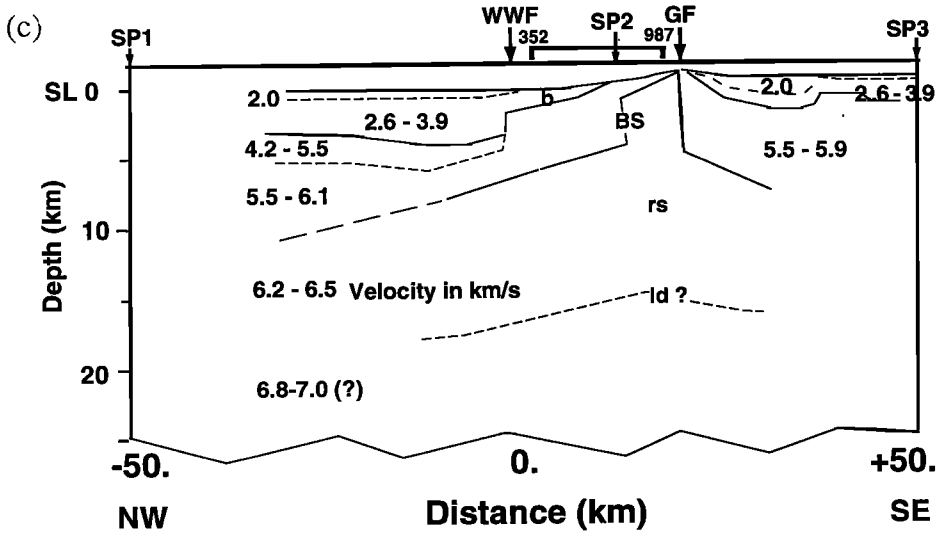

Figure 3. (continued)

continues to uplift the Tehachapi Mountains. Using these results to reconstruct the positions of the gneiss and schist in the past, it would seem that the wedge of lower crustal reflectors is related to the subcretion of the schist and subsequent tilting of the Tehachapi Mountains in latest Cretaceous/early Tertiary time.

Geological Background

Basement rocks north of the Garlock fault are exposed in scattered outcrops and consist of the 100-115 Ma Tehachapi gneiss complex and Rand schist (Figures 1 and 2) [*Pickett and Saleeby*, 1993]. These rocks once occupied the lower crust and were metamorphosed at depths of 25 to 30 km (7-10 kbar and 550 to 760°C) some 100 m.y. ago [*Saleeby*, 1990; *Jacobson*, 1990; *Jacobson et al.*, 1988; *Saleeby et al.*, 1987; *Sharry*, 1981]. Postmagmatic ductile fabrics in the gneisses are similar to those seen in the upper plates of the Vincent and Rand thrusts. These faults place intrusive rocks over the schist in the San Gabriel and Rand Mountains respectively [*Ehlig*, 1981; *Silver et al.*, 1984; *Silver and Nourse*, 1986]. Evidently, this event and its associated metamorphism took place in Late Cretaceous time [*Silver and Nourse*, 1986; *Hamilton*, 1988; *Jacobson et al.*, 1988]. On its north side, the Rand schist in the Tehachapi Mountains is bounded by a fault of variable exposure and dip that has been identified both as the "north branch" of the Garlock fault and as the "Rand thrust" [e.g., *Buwalda*, 1954; *Davis and Burchfiel*, 1973; *Burchfiel and Davis*, 1981].

Sharry [1981] has suggested that as in the case of the San Gabriel and Rand Mountains, the schist extends beyond its outcrop, perhaps even under the Tejon embayment. This possibility was discounted to some degree by *Ehlig* [1968], who suggested that only the gneiss may extend to the north. Even farther to the north, however, the basement consists of intact, shallow level batholithic crust, beneath which geophysical and deep-crustal xenolith data demonstrate that no significant underlying schist terrane exists [*Saleeby*, 1986; *Dodge et al.*, 1986, 1988]. Based on industry and COCORP seismic reflection data, *Cheadle et al.* [1986] and *Lawson* [1989] have suggested that the schist terrane is present under much of the western Mojave Desert. In terms of their upper mantles, xenolith studies from the Sierra Nevada reveal subcontinental geochemical signatures [*Mukhopadhyay et al.*, 1988], while similar studies in the eastern Mojave are more suggestive of suboceanic conditions [*Montana et al.*, 1991; *Leventhal et al.*, 1992].

The Tehachapi gneisses were rapidly uplifted to 10-15 km depth sometime between 100 and 85 Ma [*Pickett and Saleeby*, 1993]. In the Rand Mountains to the east, age and structural relations indicate emplacement of the Rand schist beneath similar crystalline rocks in this same time interval [*Silver and Nourse*, 1986]. In the Tehachapi Mountains, uplift and erosion continued into the early Tertiary, so that Eocene marine rocks of the Tejon Formation were deposited directly on the gneisses [e.g., *Goodman and Malin*, 1992]. Based on the presence of schist clasts in the "unnamed conglomerate," which overlies a major angular unconformity, the Rand schist in the Tehachapi Mountains first appeared at the surface in middle Miocene time [*Goodman*, 1989].

Geological and geophysical evidence exists for three other Oligocene to Miocene tectonic events in the Tehachapi region [e.g., *Crowell*, 1974, 1987; *Goodman and Malin*, 1988; *Goodman*, 1989; *Goodman and Malin*, 1992]. The earliest event is a late Oligocene/early Miocene period of extension, involving low- and high-angle normal faulting, volcanism, and the deposition of coarse fanglomerates. Uplift in the mid-Miocene exposed the schist and appears related to initial slip on the San Andreas fault (SAF). Extension and transtension resumed after this period, resulting in oblique slip faulting and rapid subsidence of the SSJB to bathyal depths. During late Miocene time, transtension alternated with transpression, reflected by cycles of subsidence and uplift in the SSJB. Since that time, the SSJB has evolved from submarine, to sublacustrine, to subaerial, to intermontane. Since the Pliocene, the entire region has been dominated by the transpressional regime of the modern San Andreas and Garlock faults, with local shortening taking place on features such as the WWF and Pleito thrust (Figures 1 and 2).

The left-lateral Garlock fault is the most significant and active crustal discontinuity exposed in the Tehachapi Mountains. Most of its postulated 64 km of displacement appears to have taken place since the late Miocene [*Carter*, 1987], although this fault likely originated in the mid-Tertiary [*Goodman and Malin*, 1992]. Restoration of this slip brings the Tehachapi Mountains in proximity to the western Rand Mountains (Figure 2) [e.g., *Crowell*, 1979]. Thus, if the Garlock fault is taken to be a deep, throughgoing crustal discontinuity, any model of the crust

beneath the Tehachapi Mountains must be consistent with the structure and rocks beneath the Rand Mountains.

Unfortunately, no definitive evidence on the depth of the Garlock fault presently exists. Based on the continuity of an apparent midcrustal reflector observed in the Mojave Desert COCORP data, *Cheadle* et al. [1986] proposed that the Garlock fault may not be deeply rooted (Figure 2). Alternatively, this reflector may represent a laterally displaced but flat horizon, an out-of-plane reflection, or perhaps reflected refractions from a subvertical fault [*Serpa and Dokka*, 1988]. Arrival times of refracted P_n waves show that the present Moho under the Tehachapi Mountains is flat to within a few kilometers, with no apparent differences across the surface trace of the Garlock fault [*Hearn and Clayton*, 1986b]. Midcrustal refracted P_g waves, however, show large delays across this fault, even after correction for low near-surface velocities [*Hearn and Clayton*, 1986a].

Paleomagnetic data suggest that the Tehachapi Mountains have rotated between 40° and 60° clockwise since the early Tertiary [*McWilliams and Li*, 1985]. Data from volcanic flows of early Miocene age show that as much as 40° of this rotation took place during the Neogene [*Graham et al.*, 1990; *Plescia and Calderone*, 1986]. On the other side of the Garlock fault, at sites south of the Rand Mountains, roughly 25° of Miocene clockwise rotation has been measured [*Golombeck and Brown*, 1988]. It is not known whether these rotations also apply to the Rand Mountains. In the Mojave extensional belt, *Dokka* [1989] has used paleomagnetic data and kinematic indicators to propose early Miocene north-south extension, in contrast to the more east-northeasterly direction more commonly suggested for the Mojave region.

Accepting the 40° to 60° rotations for the Tehachapi Mountains, and undoing their Neogene slip on the Garlock fault, *Goodman and Malin* [1992] argue that the mid-Tertiary extensional structures seen there are related to coeval structures in the Mojave Desert and western California. In their view, mid-Tertiary extension was regional in extent and predated, by many millions of years, deformations associated with the onshore SAF. In the Tehachapi Mountains, these mid-Tertiary features were rotated and reactivated in Neogene time.

Numerous reverse faults with differing amounts of oblique slip cut the gneiss and schist as well as the Cenozoic sediments of the

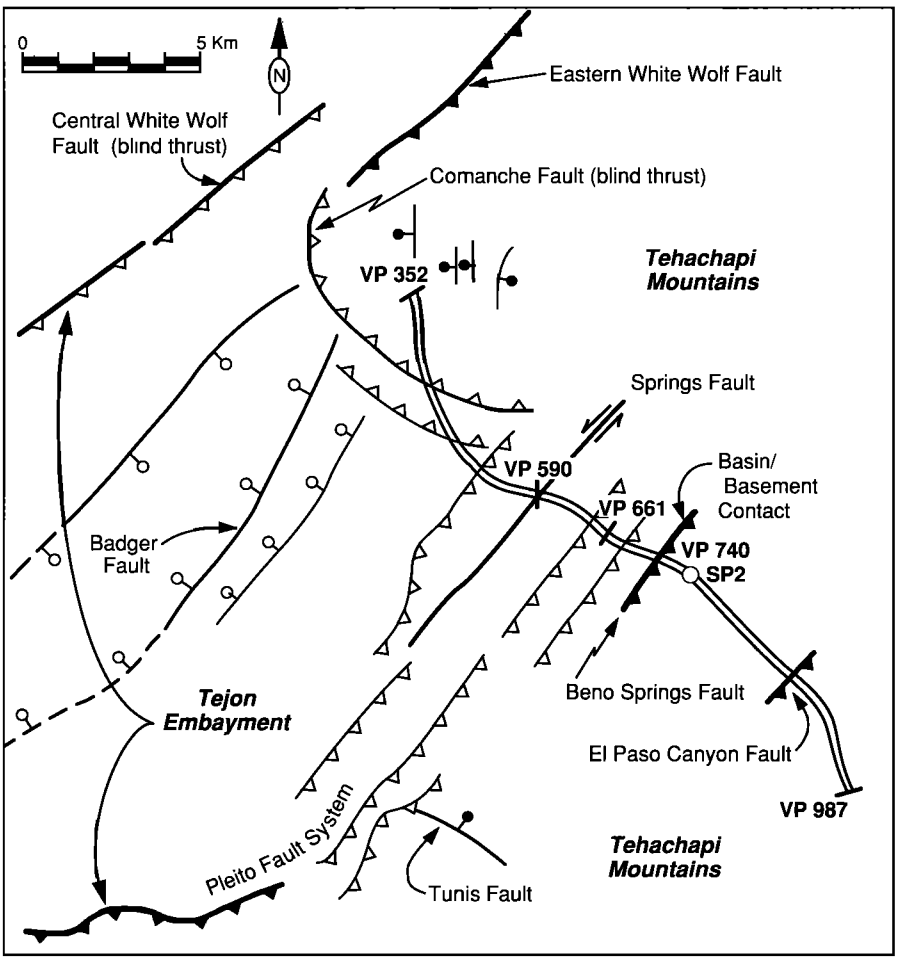

Figure 4. Fault map of the Tejon embayment and Tehachapi foothills showing the segment of the reflection survey discussed in this paper (modified from *Goodman et al.* [1989]). The faults shown include ones identified in shallow reflection data by *Goodman and Malin* [1992]. In the Tejon embayment, which lies to the northwest of VP 740, the traces of buried faults are shown with open barbs (reverse) and balls (normal); exposed faults are solid. The traces of basement/sediment contact and the Beno Springs Fault (BSF) intersect at approximately VP 740, as indicated. The WWF is segmented into exposed and buried traces near Comanche Point [*Goodman and Malin*, 1992]. The section of profile shown on this map and in Figure 6 avoids the extreme dips near the WWF (<VP 352) and severe side swipe in the narrow canyons of the high Tehachapi Mountains (>VP 987).

Tejon embayment (Figure 4). These include the WWF, Pleito thrust, and Springs faults, plus the recently recognized Comanche Point, Beno Springs, and El Paso Canyon faults [*Goodman and Malin*, 1992]. These structures, some of which may be reactivated extensional structures formed in the Oligocene and Miocene, arrived at their present configurations by the combined effects of Neogene clockwise rotation and later regional transpression. The CALCRUST data show that several of these faults played major roles in the present-day exposure of the deep-seated crustal rocks.

Seismic Reflection Data: Acquisition and Processing

The Tehachapi Mountains common midpoint (CMP) reflection profile was acquired with a contract reflection crew. The equipment used included a GEOSOURCE MDS-16 400-channel, 16-bit recorder, and six $2x10^5$ NT Litton vibrators with full force control. In the low-relief Tejon embayment, the near surface consisted of non uniformly consolidated alluvium and soil. Along the mountainous portion of the profile, access was along crooked roads in steep-sided canyons with highly variable ground surfaces, all producing undesirable types of seismic signals. Table 1 summarizes the nominal acquisition parameters that were chosen after field testing of these conditions.

Unfortunately, the tests revealed strong, site- and frequency-dependent, source coupling problems in the 18-26 Hz band. These problems produced a signal-generated artifact that obscured all reflectors below 4 s of two-way travel time (all times given here are two-way travel times). The artifact could not be effectively suppressed with changes in acquisition parameters, although numerous attempts were made. Thus even the uncorrelated field records of this survey became the subject of an independent signal-processing investigation [*Okaya et al.*, 1990, 1992]. Fortunately, the time evolution of this noise (originating possibly in the frame of the vibrator) differed from the vibrator sweep. Because of this difference it was possible to suppress the noise by filtering in a twice-transformed data domain (Table 2). The first transform took each uncorrelated field trace to its frequency-time representation. In this domain, the vibrator sweep and artifacts appear as linear functions with different slopes, like direct and refracted waves in travel time plots. The second transform operated on both the frequency and time variables (i.e., a two-dimensional transform). A simple rejection filter, analogous to a frequency-wavenumber or pie-slice filter, was then applied to these transformed data [e.g., *Yilmaz*, 1987].

A filtered shot gather from vibration point VP 661 is shown in Figure 5. This gather contains all the major reflectors seen between the WWF and Rand schist. It also shows that the signal-generated artifact was only partially removed by the special filter, perhaps due to the artifact's long duration and aliasing in time. This residual noise, plus out-of-plane reflections and reflected refractions [e.g., *Day and Edwards*, 1983], created problems in the subsequent processing. In part, because these signals have apparent moveouts similar to reflections in high-velocity basement rocks, many standard signal-enhancement procedures were not as effective as in the case of lower velocity sedimentary basins (Table 2) [e.g., *Yilmaz*, 1987] (see also Figure 7b). In the end the combination of these problems resulted in elimination of the data immediately north of the Rand schist. The most significant improvements in the final section resulted from (1) deconvolution of reverberations and multiples along with source-pulse time compression and (2) frequency-wavenumber (F-K) filtering of Rayleigh waves, s-waves, out-of-plane reflections, and reflected refractions.

After these steps, and muting of the first-break waveforms, a suite of constant velocity stacks were generated every few kilometers along the profile. These stacks helped image dipping horizons, such as the newly recognized fault zones, and identify out-of-plane events and reflected refractions. Once identified, an effort was then made to suppress the out-of-plane events and reflected refractions without affecting reflections from the dipping features (Table 2). Both migration and depth conversion tests were done on the final stack, and prestack migration was considered for critical features such as the faults and dipping zones. While helping somewhat with interpretation, the migrations resulted in sections with lower contrast and greater distortion than the depth sections. Thus, for reasons of clarity and fidelity, the latter type of section is displayed in Figure 6.

Interpretation of the Upper Crust and Moho

Vibration point VP 661 is located immediately southeast of the Springs fault basement high and where the basement surface dips to the south (Figures 4 and 5) [*Goodman et al.*, 1989;

Table 1. Data Acquisition Parameters for the Tehachapi Mountains Reflection Survey

Parameter	Nominal Values	Notes
Number of live groups	240-400 (floating)	number determined by cable roll-along rate
Roll-along configuration	split spread	40 trailing, 4 gap, 200-360 leading
Station interval	33 m	
Geophones per group	12	8-Hz geophones
Geophone array	in-line, 33 m long	
Number of vibrators	6 at 2×10^5 NT	amplitude and phase force control
Pad separation	13 m	
Vib point intervals	66-132 m	set by signal-to-noise ratio and survey costs
Vibrator array	in-line stacked	no move up due to noise on pad pickup
CMP fold	25-100	
Sweeps per station	8-12	set by signal-to-noise ratio and survey costs
Sweep frequencies	8-32 Hz	upsweep, set to reduce 18 to 26 hz harmonics
Sweep length	32 s	
Taper	2 s	
Total record length	44 s	12-s full-bandwidth listen, correlated to 14 s.

Except for geophone response and channel limits, values listed were established by field testing.

Table 2. Signal-processing Steps for the Tehachapi Mountains Seismic Reflection Survey

Step	Comments
1. Hand-edit field data and set up field statics	supply field geometry and correction velocities
2. Artifact removal	for details see *Okaya et al.* (1990, 1992)
3. Despike-deburst traces	
4. Time-frequency-amplitude analysis	in preparation for band-pass filtering
5. Global shot gather amplitude balance	
6. Time-exponential trace amplitudes	
7. Correct spherical divergence	
8. Band-pass filtering	
9. Trace autocorrelation study	in preparation for deconvolution
10. Deconvolution	
11. F-K filtering	ground roll , out-of-plane and other unwanted signals
12. Muting refractions and source noise; sort	
13. Velocity analysis and normal moveout tests	checks for out of plane events and good reflectors
14. Mute and band pass	
15. Surface-consistent residual statics tests[a]	done using pilot traces
16. Stack tests and final stack	final stacking velocities selected from suite of CV stacks
17. Time-distance dip filtering	suppression of residual unwanted signals
18. Global CMP section amplitude balance	
18. Migration tests[a]	poststack and prestack tests
18. Time to depth section conversion	
19. Final display tests	including coherency filtering, global gain, and threshold tests

For reference to the standard signal processing steps listed here, see *Yilmaz* [1987]. Editing and artifact removal completed with UCB DISCO-adapted modules. Postartifact removal processing with USC MERLIN-adapted modules.
a. Tests fail to show clearly improved stacked section due to residual artifacts.

Goodman, 1992]. The crystalline-sediment contact can be identified in the VP 661 shot gather at roughly 1 s, at the base of the zone labeled b. Progressing downward into the basement, there exists a zone of relatively flat subbasin reflectors, easily visible below 2 s, and given the label ud. These reflectors are also seen on industry seismic profiles discussed by *Goodman and Malin* [1992] and the depth sections in Figure 6.

Beneath the subbasin reflectors is the first of two major northwest dipping horizons. The upper horizon is labeled as rs in Figures 5 and 6. Near the top of this unit are phases that can be correlated over many tens of traces. Allowing for one or two waveform cycle skips, these phases can be traced across the entire shot gather (13.2 km of shot gather = 6.7 km of reflection points). The second and deeper of these two horizons, labeled m_M in Figure 5, begins just above 8 s. This second horizon is separated from the first by two other features: a zone of residual signal-generated artifacts (labeled a in Figure 5), and a zone of flat-lying, more segmented reflectors (labeled ld in Figures 5 and 6). Shot gathers to the north and south of VP 661 show that the tops of the rs and m_M horizons dip consistently northwest, moving up through the crust to the southeast. The dips of the reflectors below the m_M horizon appear to decrease with depth and grade downward to weaker, flat-lying reflections at roughly 11 s (labeled m_T in Figures 5 and 6). On other shot gathers as well as the one at VP 661, the change in dip is seen as a shift of the reflection hyperbola to shorter offsets with increasing time. In the depth section, this produces a wedge-shaped zone with a fanlike internal structure. The P_n velocities across this region [*Hearn and Clayton*, 1986b], suggest that the m_T reflectors are the current Moho. Both the P_n data and reflection data show the Moho to be flat to within 3 km.

Field mapping data plus industry seismic profiles and well logs were particularly valuable in interpreting the upper part of the CALCRUST reflection profile. For example, these data show that the Springs fault, which outcrops near VP 590 and is labeled S in Figure 6b, is part of a more complex set of structures associated with local transcurrent tectonics. Beneath VP 590 and farther to the southeast, the basin and subbasin reflectors appear to be truncated by the transcurrent structures, as is also seen in the CALCRUST profile. Near VP 661, both drill hole and shallow seismic data show buried thrust faults cutting much of the Tertiary section (these are indicated by the letter P in Figure 6b). These faults are on strike with the currently active Pleito thrust and appear to be its northeastward extension (Figure 4).

The bottom of the sedimentary basin is most prominent on the northwest end of the seismic section, and extends to a depth of 2 km there. Below this, to a depth of at least 7 km, are the ud subbasin reflectors. Both the b and ud zones rise to the south, where the sedimentary section of the Tejon embayment laps onto the crystalline rocks of the Tehachapi Mountains, at roughly VP 740 (Figure 4). The ud reflectors may be related to mid-Tertiary extensional structures (the "detachments" of *Goodman and Malin* [1992]). Basement-involving, high-angle, normal- and oblique-slip faults observed on industry data in the Tejon embayment appear to sole into similar reflectors. Outcrop data along the northern exposures of the Tehachapi gneisses suggest that they may follow older, shallow dipping, metamorphic, and ductile shear fabrics.

Two additional shallow structures have been identified on the depth section and have been confirmed in the field as faults. One is located just southeast of the sediment/basement onlap near VP 740. The other is in the gneiss complex between VP 840 and VP 860. In the depth section, these features are associated with the southeast dipping zones labeled BS and EP, which extend to depths of roughly 7 km but are difficult to see due to the scale of this section. The best images of these zones are in the constant velocity stacks shown in Figure 7. This part of the profile also appears to contain numerous out-of-plane reflections and

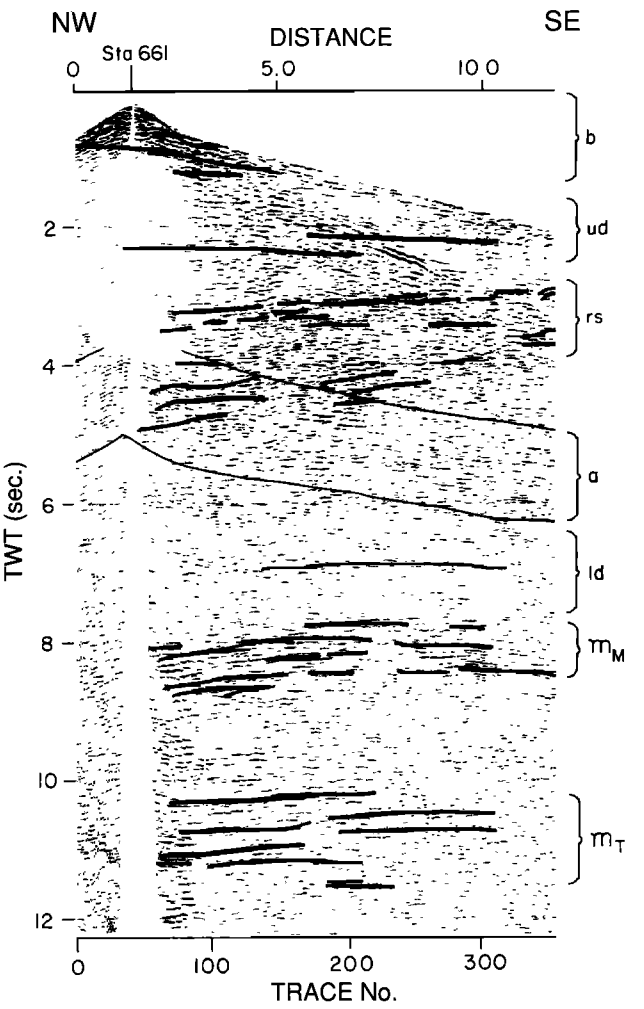

Figure 5. Prominent features in the filtered shot gather from vibration point VP 661 of the Tehachapi Mountains reflection profile, as discussed and interpreted in the text [*Okaya et al.*, 1992]. The reflection quality and continuity of the features can be judged by following the signals above and below the annotations. The annotated reflection zones are interpreted as: basin and basin bottom (b), upper detachments (ud), Rand schist (rs), acquisition artifact (a), crustal scale decollement or brittle/ductile transition zone (ld), latest Mesozoic-earliest Cenozoic ductile flow fabric or underplating or thrust zone (m_M), Tertiary Moho (m_T).

reflected refractions (labeled RR and OP in Figure 7b). Both these types of signals have high-velocity moveouts like to those of the basement rocks. Judging from local topography, geology, shot gathers, common midpoint gathers, and stacked data, the out-of-plane reflections here seem to be related to the BS and EP zones. In the stack section these signals create an appearance of crosscutting horizons [e.g., *Yilmaz*, 1987]. Taking this and the field observations into account, the southeast dipping bands are seen to be a series of coherent reflections that apparently truncate the more flat-lying reflectors, including those of the rs zone below VP 815.

Field mapping and examination of aerial photos in the area of VP 740 suggest that the dipping reflective band there is a previously unrecognized fault, which we have called the Beno Springs fault, (indicated by BS in Figures 6 and 7 and abbreviated BSF). This fault is located along a series of ridges delineated on aerial photographs. It intersects the basin/basement contact obliquely near VP 740. In the gneiss complex the fault zone consists of a 5- to 20-m-thick mylonite zone striking N50°E and dipping 50° SE. It is overprinted by cataclasite zones that dip more steeply to the southeast. The gneisses show structural and lithologic contrasts across the fault, with generally low-dipping tonalitic-dioritic gneisses in the hanging wall and refolded granitic orthogneiss and paragneiss in the footwall. From surface geology alone, a major amount of reverse displacement appear to have taken place across the BSF.

The EP zone, the El Paso Canyon fault (EPCF), reaches the surface at VP 840. Reflections from this zone are similar to those from the BSF, but the fault itself is more difficult to recognize in outcrop. Scattered exposures show a change in the attitude of foliations in the area of the reflections. West of the profile, the EPCF may form the poorly exposed contact between the Tejon Creek tonalite gneiss and the Comanche Point paragneiss units of *Sams and Saleeby* [1988].

Interpretation of Reflectors rs, ld, and m_M

The northwest dipping rs zone, the subparallel m_M zone, and the less inclined ld zone that separates them are imaged most clearly in the depth section between VP 550 and VP 815 (Figure 6). Along this portion of the profile, the top of the rs zone is between 5 and 8 km deep and has an apparent dip of 15° to 30°. From VP 450 to VP 550 this reflective zone maybe disrupted by the extension of the Pleito thrust, the Springs fault, and other interpreted blind faults, such as those interpreted beneath VP 525 and VP 400. Farther to the northwest the rs zone is identified as the weak reflectors seen in the middle crust.

South of VP 815, recognition of the rs zone in the depth section depends on (1) its signal pattern, which consists of a sharp top reflector with subparallel underlying reflectors and (2) our interpretation of the BSF and EPCF as reverse faults based on field mapping. The resulting correlation is shown in Figure 7b, with the top of the rs zone at VP 815 now appearing at a depth of less than 2 km and thrust up over its equivalent reflectors to the north. Accordingly, from both field and subsurface evidence, the BSF would have a vertical separation of almost 4 km. Farther south, on the hanging wall of the EPCF and southern end of the profile, the same assumptions suggest that the rs zone comes to within 1 km of the surface.

Giving a geological identity to the rs zone is a critical issue in interpretation of the reflection data. In this regard there are several important lines of evidence that suggest that the rs zone represents the Rand schist extending northward from its outcrop immediately to the south. First, geometric projection of the rs reflectors places them near the surface at the schist outcrop. Second, *Silver* [1982] has demonstrated the presence of stacked, north dipping thrusts with slivers of Rand schist along the Garlock fault east of the reflection profile. Third, in the San Emigdio Range immediately west of the profile, outcrop patterns of schist and gneiss also show a similar structural configuration north of the Garlock fault [*Ross*, 1985]. Further, it should be recalled that palinspastic reconstruction of the Tehachapi Mountains joins them to the Rand Mountains. In the latter mountains, the COCORP reflection data [*Cheadle et al.*, 1986] and the geological mapping data [*Silver*, 1982] show the same characteristic reflectors and rocks in this type of relationship (reflectors A, B, and G in Figure 2b, as discussed later in our reconstruction of the crustal tilting).

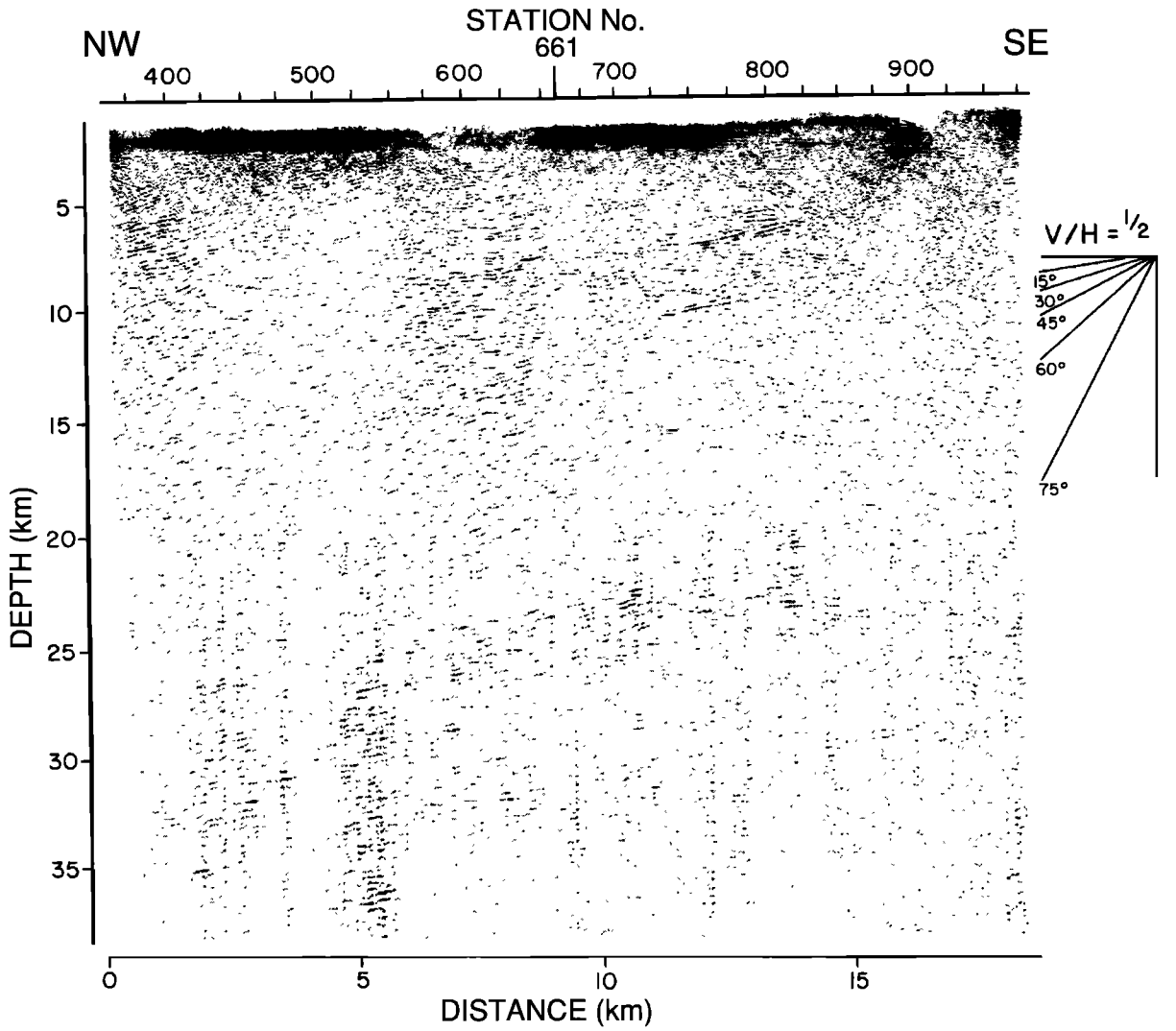

Figure 6a. This Figure shows the Tehachapi Mountains common mid-point (CMP) depth section. Plot parameters were chosen to best display the subbasin reflections discussed here (for data in the basin, see *Goodman et al.* [1989], *Goodman* [1989], and Goodman *and Malin* [1992]). In this section and the one in Figure 6b, both the stacking and display processes degraded the clearer Moho reflection seen in Figure 5. Horizontal exaggeration is approximately 2.25 to 1.

Another line of evidence comes from the refraction data and regional gravity field (Figure 3; modified from *Ambos and Malin* [1987], *Goodman et al* [1989], *Plescia* [1985], and J.B. Plescia (personal communication, 1992)). These data have been modeled using the approach suggested by *Barton* [1986]. His method uses both seismic and gravity observations, but takes into account the limits of crustal velocity-density relationships. First, the approximate geometry and composition of the sedimentary basins were entered into the model, using the refraction data, the CALCRUST and industry reflection data, and the densities given by *Plescia* [1985]. Next the depth and shape of the Moho suggested by the P_n and reflection data were used as a starting point for several models of the gravity over the Tehachapi Mountains. In these calculations, the near-surface densities assumed in the Tehachapi Mountains were those suggested by *Plescia* [1985], while the range of subsurface densities was allowed to vary within the velocity-density limits set by *Barton* [1986].

It was concluded from these tests that the depth and shape of the Moho could not vary far from that suggested by the P_n and reflection data. If true, then it is possible that the topography of the Tehachapi Mountains is gravitationally balanced within the crust alone. One way in which this balance can come about is by the presence of a slightly lighter schist body beneath the denser gneiss, in a fashion consistent with our interpretation of rs zone of reflectors being the schist. Assuming the uppermost crustal structure suggested by the reflection data, the refraction and gravity data can be fit, within the limits of their resolution, with the velocities and densities shown in Figure 3 (see caption for error limits). An important feature of the densities and layer thickness of this model is that at a depth of 32 km, the masses of the crustal columns along the profile vary by less than $\pm 1\%$ from their average, equivalent to the uncertainties in the densities and thicknesses. Thus, while not unique or definitive, the resulting gravity model fits the observed gravity within errors and is consistent with the other geophysical and geological data.

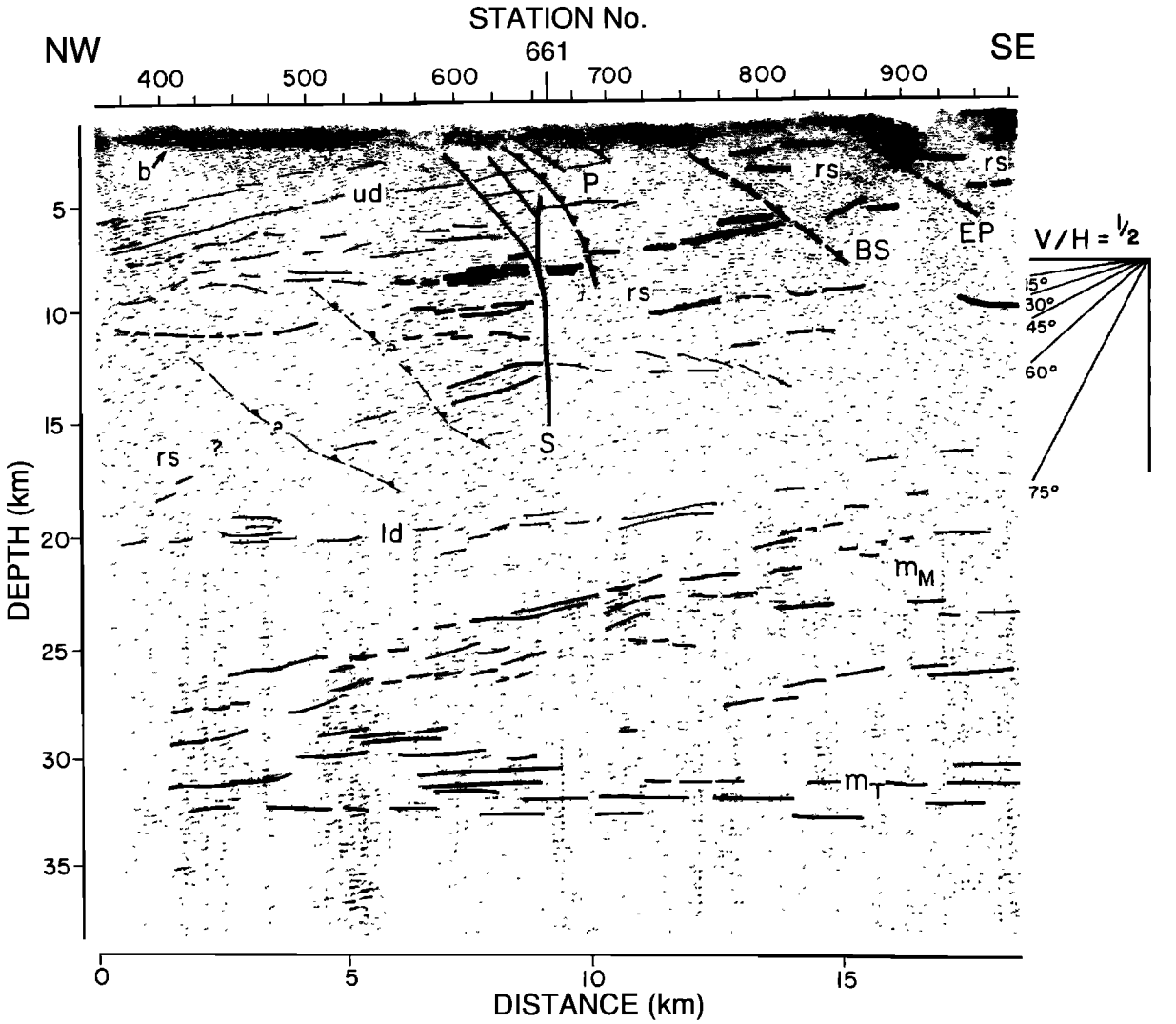

Figure 6b. Prominent features in the CMP depth section. The annotated reflection zones used here are the same as those interpreted in Figure 5. Additional interpreted structures are Springs fault (S), Pleito thrust (P), Beno Springs fault (BS), El Paso Canyon fault (EP).

The main discrepancy in our refraction model is with previous work by *Malin et al.* [1981], who profiled the velocity structure of the schist at Sierra Pelona in the San Gabriel Mountains. They found the schist *P* velocity to be around 5.9 km/s as compared to the 6.2–6.5 km/s values shown in Figure 3. This difference maybe due to pressure, the 5.9 km/s being determined at a depth of roughly 1 km and the 6.2-6.5 km/s at roughly 10 km. In fact, if the schist extends below Sierra Pelona to these depths, where *Malin et al.* [1981] found similar velocities, then no discrepancy exists. The difference may also reflect anisotropic velocities in the schist.

Thus the evidence at hand suggests that the rs zone is the Rand schist, that its top is the Rand thrust, and that its internal reflections are a function of changes in structural fabric, compositional layering, and tectonic imbrication and duplication. Nonetheless, because the reflection line failed to carry the rs zone to outcrop, there remains some doubt: the rs zone could represent internal structure within the Sierra Nevada batholith or an entirely unknown horizon. In particular, if the rs zone is within the batholith, it could be associated with some type of imbrication, placing higher level rocks under the gneisses. Another possibility is that while the rs zone is the schist, it may exist as a thin sliver, only 2 or 3 km thick, sitting on an entirely unknown or unrelated basement. Such interpretations could also satisfy the gravity and refraction data, particularly if the rocks beneath the gneisses are relatively light and fast. These possibilities are kept in mind in our uplift model. As a final note on rs, if our correlation is correct, the steeply dipping contacts on the north side of the schist outcrop may be south dipping faults similar to the BSF and EPCF.

In the depth sections in Figure 6, the ld zone seems to mark a transition from a more reflective but less laterally coherent upper crust to a less reflective but more laterally coherent lower crust. Below the ld zone, at VP 740, is the top of the m_M zone, at a depth of roughly 22 km and dipping 25°N. While less clear than in the shot gathers, the reflectors below this horizon appear to flatten with depth to the less distinct Moho m_T. The CMP stacking process degraded the m_T zone so much that shot gathers were used to help identify it in Figure 6. To some degree, the wedge of lower crustal reflectors bounded by m_M and m_T resembles a fan with its hinge point to the northwest of the profile. The same kind of reflection structure was also observed

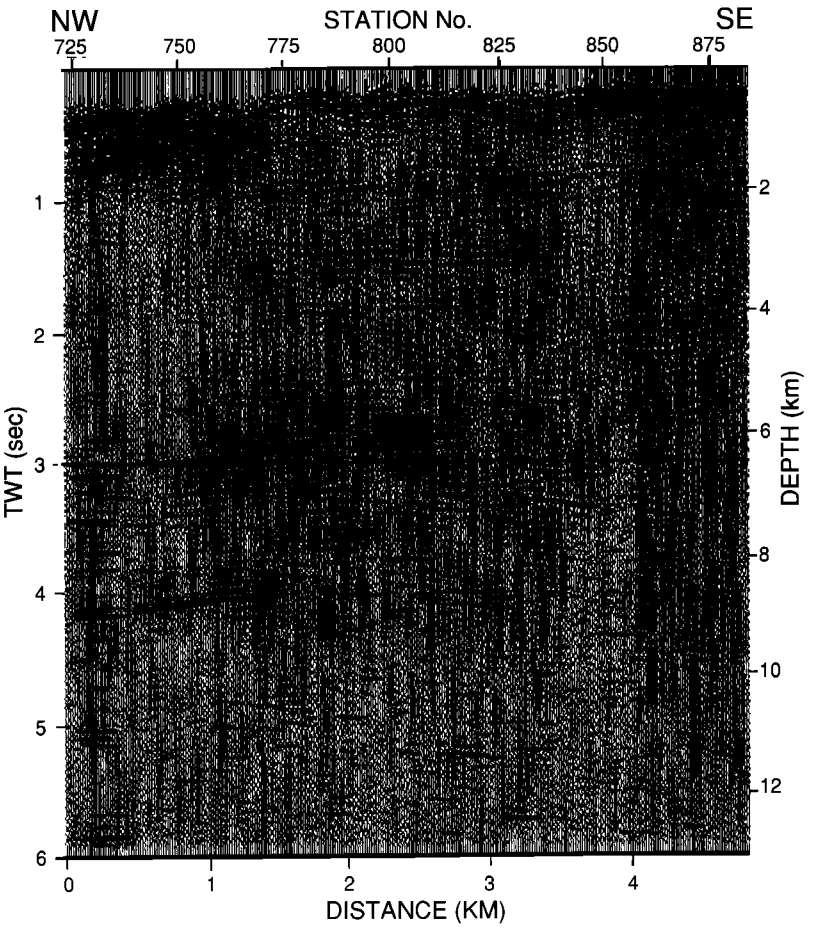

Figure 7a. Expanded-scale constant velocity (5.6 km/s) stack of the CMP data from the areas of the Beno Springs and El Paso Canyon faults (VP 720 to VP 885). The horizontal exaggeration is approximately 2.25 to 1. This section allows for the presence of high-velocity gneiss, schist, and the moderately to steeply dipping fault zone reflections immediately below VP 740 and VP 850. The section contains out-of-plane reflections from this fault that appear to cross some of the more flat-lying reflectors. The section also contains residual reflected-refractions above the rs horizon.

at the eastern end of Mojave Desert line 3, beneath and just south of the Rand Mountains, but with a different geographic orientation [*Cheadle et al.*, 1986] (reflectors I and M, as shown in Figure 2).

As stated earlier, the P_n data of *Hearn and Clayton* [1986b] show mT to be a horizontal Moho. As in many other places, this particular Moho is a complex zone with numerous discontinuous phases that can be seen in shot gather but do not stack into a single coherent horizon [e.g., *Mereu et al.*, 1989]. A common model for the zone of flat, superimposed lenses of discontinuous reflectors is differentiation and underplating of the lower crust by partial melting of the upper mantle [e.g. *Hauser et al.*, 1987]. Likewise, the ld horizon has numerous analogs in which a laminated lower crust is separated from a heterogeneous upper crust [e.g., *Mereu et al.*, 1989]. The differences above and below this horizon may be products of brittle versus ductile deformation. The deformations could be related to the current seismotectonic regime in southern California and/or to the events that rotated the Tehachapi Mountains earlier in the Neogene. As in the case of the upper detachment horizon, ud, which can account for differences in the structural styles of the sedimentary section versus underlying basement, interpretation of ld as a lower decollement helps to explain some differences between the upper and lower crust.

Exposure of the Gneiss and Schist

For a plausible geological explanation of the Tehachapi Mountains reflection profile and other data, we have assumed the following statements to be true:

Basic Relationships

1. The Tehachapi gneisses correspond to southward deepening exposure of the Cretaceous Sierra Nevada batholith [e.g., *Ross*, 1985, 1989; *Saleeby* 1990].

2. The Rand schist extends northward beneath the Tehachapi gneisses [e.g., *Sharry*, 1981].

3. The schist is present under large parts of the western Mojave Desert [e.g., *Lawson*, 1989].

4. The Garlock fault is a deep-rooted crustal boundary that is more or less vertical [e.g., *Hearn and Clayton*, 1986a, b].

Basic Sequence of Events

1. The protolith of the schist was emplaced and metamorphosed under the gneiss in the Late Cretaceous [e.g., *Silver and Nourse*, 1986].

2. Substantial uplift and cooling of the schist and overlying gneisses took place during the Late Cretaceous and continued into Paleocene time [*Pickett and Saleeby*, 1993].

3. Following erosion of the gneisses and overlying crust,

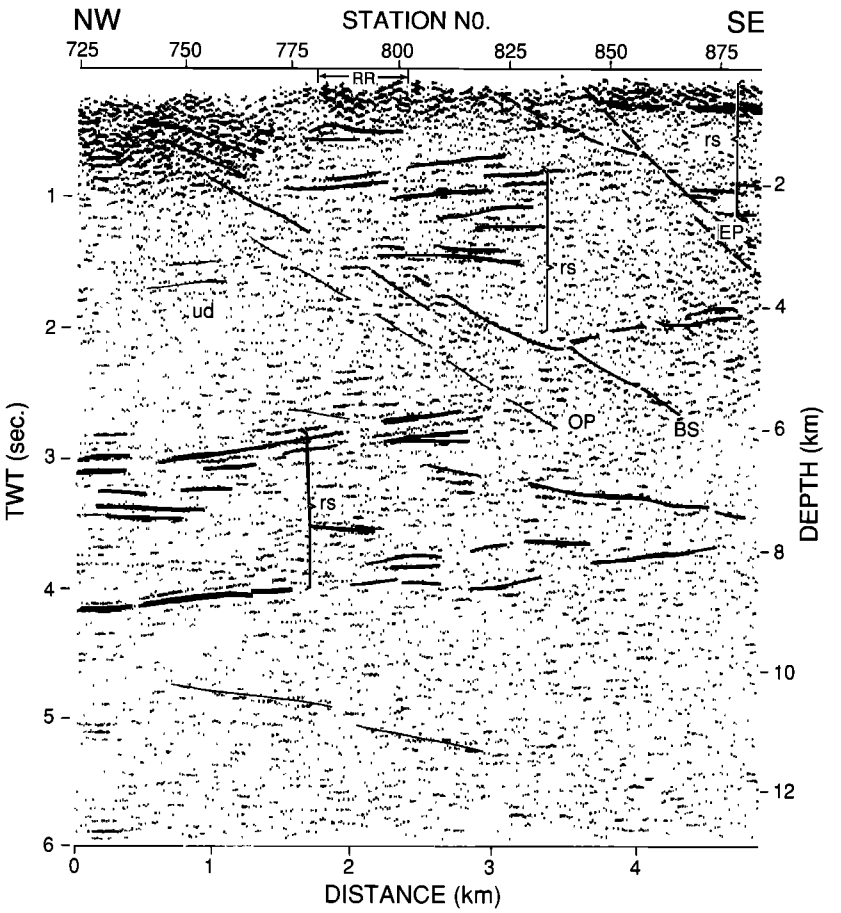

Figure 7b. Interpretation of this CMP section after application of a coherency filter and plotting signals above a minimum amplitude threshold. The annotated reflection zones used here are the same as those in Figure 6: reflectors within the Rand schist and whose top would be the Rand thrust (rs), Beno Springs fault (BS), El Paso Canyon fault (EP). Out of plane reflections (OP) cross the subhorizontal rs reflectors at high angles and are related to the BSF and EPCF. Reflected refractions (RR) produce the herring bone pattern at the top of the section.

Eocene marine sediments were deposited onto the gneisses; sediment onlap was to the east in terms of present-day coordinates [e.g., *Goodman*, 1989; *Goodman and Malin*, 1992].

4. Formation of Oligocene/Miocene basins by extension/transtension [e.g., *Crowell*, 1987].

5. Major uplift in the mid-Miocene (~17 Ma) at about the time the modern San Andreas fault became active in central California [*Goodman and Malin*, 1992].

6. The Tehachapi Mountains were apparently rotated between 30° and 45° clockwise during the Neogene, after substantial uplift of the schist and gneisses, and possibly another 30° earlier [e.g., *McWilliams and Li*, 1985; *Plescia and Calderone*, 1986].

7. The Rand schist in the Tehachapi mountains was first exposed in mid-Miocene, as indicated by clasts in the Unnamed conglomerate [*Goodman*, 1989].

8. Left-lateral slip on the Garlock fault in the late Miocene followed the rotations and separated the schist bodies now exposed in the Tehachapi and Rand Mountains [e.g., *Carter*, 1987].

9. Regional contraction and local transpression beginning in the late Pliocene further exhumed the schist [e.g., *Graham et al.*, 1990]. The schist is now exposed at scattered outcrops along the San Andreas, San Gabriel, and Garlock faults (Figure 2a) [e.g., *Ehlig*, 1968].

Since basic relationships 2, 3, and 4 have not been established beyond a reasonable doubt, it is also necessary to consider the following possibilities to be true.

Alternative Relationships

1. The schist is not present immediately beneath the Tehachapi gneisses or large parts of the Mojave [e.g., *Ehlig*, 1968, 1981]. The crust beneath these regions consists of imbricated high level intrusive rocks of the Sierra Nevada Batholith or some other unit.

2. The Garlock fault is not a deep-rooted, vertical crustal boundary. Beginning with our basic set of assumptions and moving backward in time, the following reconstruction of the crust below the Tehachapi Mountains is proposed. Undoing the Neogene left-lateral slip of the Garlock fault brings the reflection structure of the Tehachapi Mountains adjacent to that of the Rand Mountains (Figure 2) [*Carter*, 1987]. By their timing, the Neogene tectonic and depositional events in the SSJB seem related to the rotations established by paleomagnetism for the general Mojave region [e.g., *Graham et al.*, 1990]. In the same vein, faults like those shown in Figure 4 and/or a midcrustal decollement may have accommodated the necessary upper crustal extension and shortening as the rotations progressed [*Goodman and Malin*, 1992; *Jackson and Molnar*, 1990, Figure 3; *Ingersoll*, 1988]. Owing to the rotations and onset of SAF-related tectonics, north directed reverse faulting became active and stepped

northward toward the Tejon embayment. The structurally highest reverse faults locally exhumed the Rand schist in their hanging walls in mid-Miocene time. The pre-Garlock Neogene rotations may have occurred above the interpreted decollement ld so that the deeper reflectors m_M and m_T are in their original orientations. If so, they may directly relate to the deep reflectors observed south of the Garlock fault and beneath the Rand Mountains. The most straightforward correlation is to identify horizons ld, m_M, and m_T of this study with COCORP horizons F, I, and M respectively (Figure 2b) [*Cheadle et al.*, 1986].

Since the rotational history of the Rand Mountains is not known, direct correlation of upper crustal features across the Garlock are difficult. We suggest that the rs zone in the Tehachapi Mountains and reflectors A, B, and G in the Rand Mountains are related (Figures 2 and 6). We have also proposed that the top of the rs zone corresponds to the Rand thrust. *Cheadle et al.* [1986] have made the same correlation with COCORP reflector A. Both rs and A horizons have been interpreted as being cut by high-angle structures, which in the Tehachapi Mountains profile have been established as reverse faults.

In any case, it appears that the Rand schist and overlying rocks in the Tehachapi and Rand Mountains were uplifted together in a single event that took place near the Cretaceous/Paleocene boundary [*Silver and Nourse*, 1986; *Jacobson et al.*, 1988; *Pickett and Saleeby*, 1993]. The questions raised by this event include (1) the mechanics of the uplift and (2) the removal of the overlying upper crust. If the schist is present under the batholithic basement of the western Mojave there is the additional question of (3) the removal of the original lower crust and mantle. Central to these issues are the nature of the lower crustal reflectors that lie beneath these mountain ranges.

Presently, interpretations of the deep reflection structure along the Tehachapi Mountains and Mojave Desert profiles offer two end-member scenarios for the unroofing of the schist and overlying gneiss. The first scenario is our preferred working model for explaining the exposure of the deep-crustal rocks and its related lower crustal evolution. This model consists of Late Cretaceous eastward underthrusting of the Rand schist with resulting crustal thickening, followed immediately by gravitational collapse and isostatic crustal unloading [cf. *Burchfiel*, 1992]. The late Cretaceous/early Tertiary unloading event would have been accompanied by brittle and ductile deformation, including low-angle faulting, large-magnitude lower crustal flow and, possibly, magmatic underplating (modified from *Wernicke and Axen* [1988] and *Block and Royden* [1990]). The reflection structures between m_M and m_T in the CALCRUST data (Figure 6) and I and M in the COCORP data (Figure 2) are interpreted as developing along the margins of thick sections of subcreted schist, and hence along the margins of extended crust. These wedges of lower crustal reflectors are related to the crustal-scale tilting pattern observed in the Tehachapi and Rand mountains, including intracrustal support of their topography. We propose that the internal fan character of the wedges is a result of either ductile flow layering and/or progressive magmatic underplating of the tilting margin. In the case of ductile flow, the reflection fabric developed as material moved up and away from the margin, while in the case of underplating successive magmatic units participated in the tilting. In either case, the schist was then brought to the surface at a much later time. In the upper crust, extension was probably accommodated along stacks of low-angle normal faults [cf. *Wernicke and Burchfiel*, 1982]. Conclusive field evidence for normal faults of this age does not yet exist, but they may not have been recognized because of their reactivation in the Neogene (e.g., Pastoria thrust, Figure 1; as discussed below).

In the second scenario, which is more in keeping with the alternative relationships listed above, the reflectors m_M and I (or possibly F, as proposed by *Cheadle et al.* [1986]) represent regional thrust ramps that sole into the reflection Moho and along which the gneiss and schist were carried to the surface. In such fold-and-thrust belt models for exposure of the deep crust, the overlying crust is usually considered to have been removed by erosion. The current reflection Moho, m_T and M, would then also be tectonic boundaries, since m_M and I appear to sole into them. Finally, if the Garlock is not a deep crustal boundary, these reflectors may not even be spatially related.

In this model, the reflectors within rs could be parts of the thrust system and the gneiss and schist bodies could be of only local significance (i.e., structurally unrelated to any of the other schist exposures shown in Figure 2). A major problem with this interpretation is that a thrust ramp of this magnitude should have some surface geological expression, (an obvious outcrop or terrane boundary) none of which has been found to date. There would also be a major puzzle as to what underlies the schist and allows for the degree of observed uplift. Also missing is a sedimentary record of the proper age and paleogeographic setting for the deposition of the eroded overburden.

A Crustal-Scale Tilting Model

Regional tectonic relationships in southern California help constrain the crustal unloading and tilting model that we propose for the exposure of deep crustal rocks in the Tehachapi Mountains. All the available evidence indicates that the Rand and correlative schists were thrust beneath Tehachapi-style gneisses and intrusive rocks of the Cordilleran batholithic belt in Late Cretaceous time [*Silver and Nourse*, 1986: *Hamilton*, 1988; *Jacobson et al.*, 1988]. The east-west continuity of the upper plate geology in southern California requires emplacement of the ensimatic schist terrane by underthrusting from the west. This subcretion event corresponds in time with the initiation of Laramide, rapid, low-angle subduction [*Dickinson and Snyder*, 1978; *Bird*, 1988; *Hamilton*, 1988]. In our proposed crustal-scale tilting model, emplacement of the schist terrane initiated crustal collapse by the addition of a buoyant plate of varying thickness to the lower crust. The observed low-angle ductile flattening fabrics within schist exposures, conflicting kinematic indicators along the faults above the schist, and the evidence for latest Cretaceous/Paleocene low-angle normal faulting suggest that the crust collapsed shortly after the emplacement of the schist [e.g., *Haxel et al.*, 1985; *Nourse and Silver*, 1986; *Hamilton*, 1988; *Jacobson et al.*, 1988; *Nourse*, 1989]. Tilting and doming of the deep-level, Tehachapi/Rand basement rocks occurred in this setting. Given the disappearance of these rocks to the north [e.g., *Ross*, 1985, 1989; *Saleeby*, 1986; *Dodge et al.*, 1986, 1988; *Saleeby*, 1990], they also appear to sit on its northern edge. This picture is also supported by differences in upper mantle geochemistry north and south of the Garlock fault [*Mukhopadhyay et al.*, 1988; *Montana et al.*, 1991; *Leventhal et al.*, 1992].

Figure 8 summarizes in a series of schematic cross sections our model for subcretion of the schist, the extensional unloading event, the tilting of the Tehachapi Mountains, and Eocene

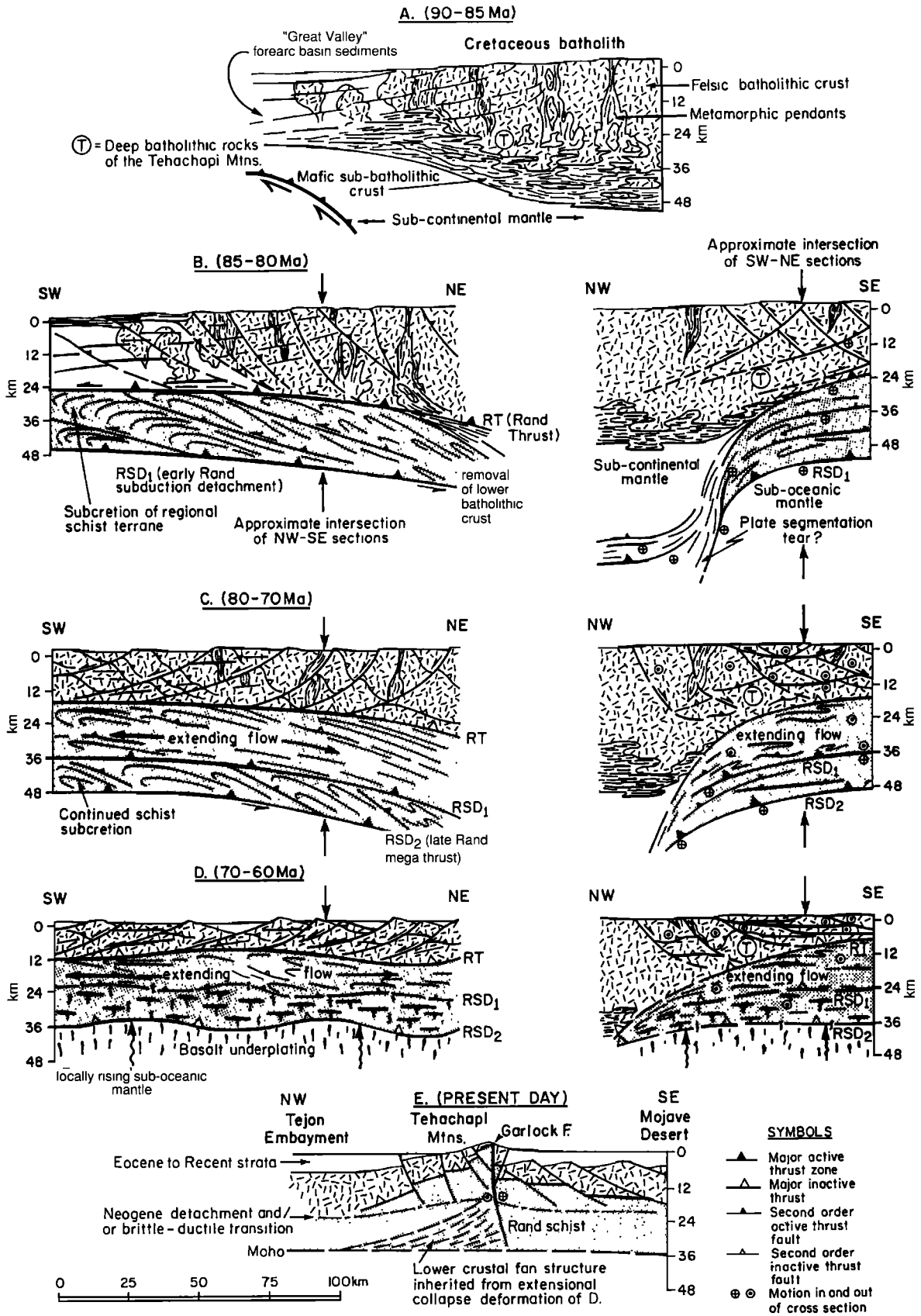

Figure 8. This Figure shows a schematic summary of the subcretion and extensional collapse model for the restored Tehachapi and Rand Mountains regions. (a) Generalized starting conditions of the batholithic crust with the approximate location of the deep-level Tehachapi rocks indicated. (b)-(d) Orthogonal views during the crustal evolution that has exposed the deep-crustal metamorphic core of the Tehachapi and Rand Mountains. (e) The current configuration of the crust. The intersections of views are as indicated in Figure 9. Extensional collapse structures were favorably oriented for reactivation as reverse faults during either Tertiary crustal rotations or Pliocene to Recent contraction. (For additional evidence for NW-SE differences shown in the crust see *Ross* [1985, 1989], *Saleeby et al.* [1987], *Dodge et al.* [1986, 1988], and *Saleeby* [1990].)

exposure of their metamorphic core. The model begins 90 to 85 Ma with a Sierra Nevadan batholith that was flanked to the west by a forearc basin. The thickness of the batholithic crustal is assumed to be ~50 km, with an increase in mafic rocks with depth [e.g., *Saleeby*, 1990]. The increase in mafic rocks is indicated by the presence of mafic lower crustal xenoliths in the upper parts of the batholith [*Dodge et al.*, 1986, 1988] and deep exposures along its tilted north-south axis [*Saleeby*, 1990]. The structure of the batholithic belt during this time interval is assumed to have been two-dimensional along the present Sierra Nevada and Mojave Desert.

Figure 8 shows two orthogonal cross sections of the initial underthrusting of the Rand schist at 85 to 80 Ma [*Jacobson*, 1990; *Silver and Nourse*, 1986]. A low-angle segment of the subducting oceanic plate carried the ensimatic schist protolith beneath the batholithic belt at lower crustal levels. The deepest and most mafic layers of the Sierran batholith were thus displacement down dip along the subduction zone. Regional magmatic activity may have ended in this initial underthrusting phase. Likewise, the beginning of broad uplift with compressional faulting might have destroyed the adjacent forearc basin. To account for the northward disappearance of the schist, zonation of the batholith, and geochemical and geophysical differences, the NW-SE cross sections show the northern terminus of the subcreted schist terrane at the latitude of the Tehachapi Mountains and Tejon embayment.

From Late Cretaceous (80 to 70 Ma) to latest Cretaceous/early Paleocene (70 to 60 Ma), we show the schist protolith as a water-rich, accretionary body beneath the upper plate batholithic crust. Under these conditions, the subcreted rocks were highly ductile; the fluids that escaped upward from them weakened the quartz-rich upper plate and promoted retrograde metamorphic reactions in it [e.g., *Wernicke*, 1990]. The tectonically thickened crust then collapsed under its own burden. This collapse was facilitated by horizontal flow within the newly formed schist and fragmentation of the upper plate into shallow dipping slabs bounded by ductile/brittle shear zones. We propose that the integrated displacement of these slabs was to the west (modified from *Silver* [1983] and *May* [1989]). During this westward transport, the crystalline rocks of the Tehachapi Mountains may have undergone up to 30° of clockwise rotation [*Burchfiel and Davis*, 1981; *McWilliams and Li*, 1985; *Plescia and Calderone*, 1986].

During the collapse phase, magmatic underplating may have occurred, at least locally. Igneous-textured, lower crustal mafic xenoliths with mid-ocean ridge basalt (MORB) isotopic signature and latest Cretaceous/early Paleocene ages are present in eastern Mojave volcanic flows [*Montana et al.*, 1991; *Leventhal et al.*, 1992]. This is consistent with subcreted oceanic mantle supplying the melts. Figure 8 shows the underplating as an important feature during the late phases of extensional collapse, subsequent to the underthrusting of the oceanic plate.

In summary, we propose that crustal-scale tilting of the Tehachapi Mountains is related to the removal of the deepest levels of the Sierran batholith by subcretion and imbrication of the schist and subsequent extensional collapse and magmatic underplating. The regional setting suggests that the tilting took place along the northern boundary of this process. Thus the m_M to m_T wedge of reflectors may be analogous to the ductile flow and shear layering commonly developed around the edge of a ductile boudin, in this case, a crustal-scale boudin of subcreted schist. Progressive, late stage underplating, which should accompany the extensional collapse, may also contribute to the reflection character of the wedge.

Implications for Regional Reconstruction

As type localities for gneissic and schistose rocks, the Tehachapi and Rand Mountains present a unique opportunity for reconstructing the manner in which such rocks might be uplifted from the lower crust. South of the Tehachapi and Rand Mountains, exposures of deep plutonic rocks and coincident lower plate schist are found in southeastern California and southwestern Arizona (Figure 2). Structural relations and seismic data suggest that large tracts of the schist underlie the Mojave Desert [e.g., *Silver*, 1982; *Cheadle et al.*, 1986; *Lawson*, 1989]. In contrast, no schist exposures occur in the Peninsular Ranges batholith, southwest of the current SAF in the Mojave Desert. A

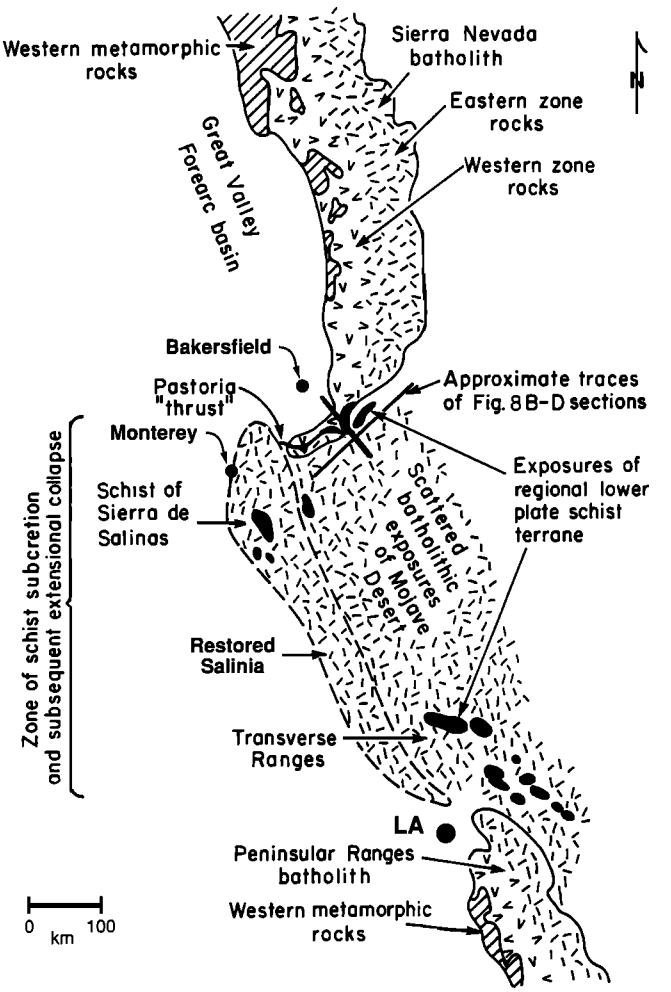

Figure 9. A diagrammatic map restoration showing pre-Neogene distribution of upper plate sialic crystalline rocks and lower plate schist exposures relative to the Sierra Nevada and Peninsular Ranges batholiths (modified from *Burchfiel and Davis* [1981]), as compared to the present-day schist distribution shown in Figure 2. Salinia is suggested to have been dispersed westward from a subcretion-extension zone [after *Silver*, 1983; *May*, 1989; *Silver and Nourse*, 1986] with the lower plate schist terrane possibly represented by the schist of Sierra de Salinas [*Ross*, 1976]. The transverse petrochemical zonation pattern of batholithic belt is that of *Silver et al.* [1979], *Mattinson and James* [1985], *Silver and Mattinson* [1986], and *Saleeby* [1990]. The margins of the Mesozoic schist bodies later served to localize major Neogene structures that dismembered and exposed relatively small portions of the schist itself.

reconstruction of upper plate, sialic crystalline rocks and lower plate schists before slip on the SAF and Garlock fault places the Salinian crystalline terrane west of our postulated extensional collapse zone (Figure 9; modified from *Burchfiel and Davis* [1981]). Since Salinia appears on its north end to be part of the Sierra Nevada and on its south end part of the Peninsular Ranges [*Silver and Mattinson, 1986*], our preferred model suggests that it was brought westward from them by the extension following the subcretion of the schist (modified from *Silver* [1983], *May* [1989], and *Silver and Nourse* [1986]).

In support of this idea, we note that after unslipping the Neogene faults, the width of the Cretaceous batholith in the Mojave is at least twice that of the southernmost Sierra Nevada and the northernmost Peninsular Ranges. This expanded segment is coincident with the lower plate schist exposures (Figure 9). Rocks that are typical of the eastern zones of the batholithic belt appear in the west along the expanded segment [*Mattinson and James*, 1985; *Silver and Mattinson*, 1986]. An example of this extension may be preserved in the Tehachapi Mountains. Here, younger, eastern zone, high-level granitic rocks lie above older, western zone, deep-level tonalitic and dioritic gneisses along the Pastoria fault [*Crowell*, 1974; *Ross*, 1989]. The geometry of the Pastoria fault and its kinematic indicators are complex, but dramatic upper plate/lower plate contrasts across it are consistent with large normal separation, resulting in the upper-plate rocks moving westward in the early Tertiary (Figures 1 and 9).

Moreover, the metamorphic wall rocks of the batholithic belt that should now lie on the western margin of the expanded belt appear to be missing (Figure 9), so is the corresponding forearc basin. Destruction of the metamorphic belt and the forearc basin along this segment of the batholithic belt may have occurred as a result of underthrusting of the schist protolith and westward denudation during postsubcretion extension.

In our model, the expanded segment of the Sierra Nevada batholithic belt corresponds to the region of schist subcretion and extensional collapse and is a product of that process. We suggest that the rapidly subducting oceanic plate was segmented into fault-bounded domains of different dips, similar to the modern Nazca plate [*Barazangi and Isacks*, 1976]. In this model, the schist-subcretion zone in the lower crust corresponds to a shallow-dipping segment of the subducting plate. The crust of the modern Tehachapi and Rand mountains was apparently situated near the northern edge of this low-dipping plate segment. As a result of schist emplacement and extensional collapse, this region was strongly tilted, exposing the roots of the Sierras and later the lowerplate schist itself.

Acknowledgments. This work was supported under NSF grants EAR83-19254 to CALCRUST, EAR87-08266 and 89-04063 to J. Saleeby, and EAR91-19263 and 91-19263 to P. Malin. J. Plescia of the Jet Propulsion Laboratory, Pasadena, California, provided gravity data and several early models from which Figure 3 was developed. We are grateful for his open and kind help. The authors have benefited from conversations with J. Crowell, T. McEvilly, S. Richard, and J. Sharry and many others. We would like to thank ARCO for providing their "vibrator buster" test equipment to check the vibrators before the survey and the Tejon Ranch Company for access to their property in the Tehachapi Mountains. We thank E. Karageorgi for generating the filtered field data at the Earth Science Division, Lawrence Berkeley Laboratory. Comments on the original manuscript by L. Serpa, T. Broecker, and an anonymous reviewer are gratefully acknowledged. Further constructive reviews, resulting in the present manuscript, were provided by E. Hauser, G. Fuis, and T. Pratt. Three thoughtful and knowledgeable reviews by G. Fuis were especially appreciated.

References

Ambos, E. L., and P. E. Malin, Combined seismic reflection/refraction investigation in the Tehachapi Mountains, southern California: Results from the 1986 CALCRUST experiment, *Eos Trans AGU, 68* (44), 1360, 1987.

Barazangi, M., and B. L. Isacks, Spatial distribution of earthquakes and subduction of the Nazca plate beneath South America, *Geology, 4*, 686-692, 1976.

Barton, P. J., The relationship between seismic velocity and density in the continental crust – A useful constraint?, *Geophys. J. R. Astron. Soc., 87*, 195-208, 1986.

Bird, P., Formation of the Rocky Mountains, western United States: A continuum computer model, *Science, 239*, 1501-1507, 1988.

Block, L., and L. H. Royden, Core complex geometries and regional scale flow in the lower crust, *Tectonics, 9*, 557-567, 1990.

Burchfiel, B. C., Extension contemporaneous with shortening within mountain belts, *Geol. Soc. Aust. Abstr., 32*, 6-8, 1992.

Burchfiel, B. C., and G. A. Davis, Mojave Desert and environs, in *The Geotectonic Development of California*, Rubey Volume 1, edited by W. G. Ernst, pp. 217-252, Prentice-Hall, Englewood Cliffs, N. J., 1981.

Buwalda, J. P., Geology of the Tehachapi Mountains, California, *Bull. Calif. Div. Mines, 170*, 100 pp., 1954.

Carter, B., Quaternary fault-line features of the central Garlock fault, Kern County, California, *Field Trip Guideb. 57*, 67 pp., Soc. of Econ. Paleontol. and Mineral., Pac. Sect., Bakersfield, Calif., 1987.

Cheadle, M. J., B. L. Czuchra, T. Byrne, C. J. Ando, J. E. Oliver, L. D. Brown, S. Kaufman, P. E. Malin, and R. A. Phinney, The deep crustal structure of the Mojave Desert, California, from COCORP seismic reflection data, *Tectonics, 5*, 293-320, 1986.

Crowell, J. C., Origin of late Cenozoic sedimentary basins in California, *Spec. Publ. Soc. Econ. Paleontol. Mineral., 22*, 190-204, 1974.

Crowell, J. C., The San Andreas fault system through time, *J. Geol. Soc. London, 136*, 293-302, 1979.

Crowell, J. C., Late Cenozoic basins of onshore southern California: Complexity is the hallmark of their tectonic history, in *Cenozoic Development of Coastal California*, Rubey Volume VI, edited by R. V. Ingersoll and W. G. Ernst, pp. 207-241, Prentice-Hall, Englewood Cliffs, N. J., 1987.

Davis, G. A., and B. C. Burchfiel, Garlock fault: An intra-continental transform structure, southern California, *Geol. Soc. Am. Bull., 84*, 1407-1422, 1973.

Day, G.A. and J.W.F. Edwards, Reflected refracted events on seismic sections, *First Break*, September 1983, 14-17, 1983.

Dickinson, W. R., and W. Snyder, Plate tectonics of the Laramide orogeny, *Mem. Geol. Soc. Am., 151*, 355-366, 1978.

Dodge, F. C. W., K. C. Calk, and R. W. Kistler, Lower crustal xenoliths, Chinese Peak lava flow, central Sierra Nevada, *J. Petrol., 27*, 1277-1304, 1986.

Dodge, F. C. W., J. P. Lockwood, and L. C. Calk, Fragments of the mantle and crust from beneath the Sierra Nevada batholith: Xenoliths in a volcanic pipe near Big Creek, California, *Geol. Soc. Am. Bull., 100*, 938-947, 1988.

Dokka, R. K., The Mojave extensional belt of southern California, *Tectonics, 8*, 363-390, 1989.

Ehlig, P. L., Causes of distribution of Pelona, Rand, and Orocopia schist along the San Andreas and Garlock faults, in Proceedings of the Conference on Geological Problems of the San Andreas Fault System, edited by W. R. Dickinson and A. Grantz, *Stanford Univ. Publ. Geosci., 11*, 294-305, 1968.

Ehlig, P. L., Origin and tectonic history of the basement terrane of the San Gabriel Mountains, central Transverse Ranges, in *The Geotectonic Development of California*, edited by W. G. Ernst, pp. 253-283, Prentice-Hall, Englewood Cliffs, N. J., 1981.

Golombeck, M., and L. Brown, Clockwise rotation of the western Mojave Desert, *Geology, 16*, 126-130, 1988.

Goodman, E. D., The tectonics of transition along an evolving plate margin — Cenozoic evolution of the Southern San Joaquin Basin,

California, Ph.D. thesis, 225 pp. and 3 plates, Univ. of Calif., Santa Barbara, 1989.

Goodman, E. D., and P. E. Malin, Comments on the geology of the Tejon embayment from seismic reflection, borehole and subsurface data, in *Studies of the Geology of the San Joaquin Basin, Publ. 60*, edited by S. A. Graham, pp. 89-108, Pacific Section, Society of Economic Paleontologists and Mineralogists, Bakersfield, Calif., 1988.

Goodman, E. D., and P. E. Malin, Evolution of the southern San Joaquin Basin and mid-Tertiary transitional tectonics, central California., *Tectonics, 11*, 478-498, 1992.

Goodman, E. D., P. E. Malin, E. R. Ambos, and J. C. Crowell, The southern San Joaquin Valley as an example of Cenozoic basin evolution in California, in *The Origin and Evolution of Sedimentary Basins and their Energy and Mineral Resources, Geophys. Monogr. Ser.*, vol. 48, edited by R. A. Price, pp. 87-107, AGU, Washington, D. C., 1989.

Graham, S. A., P. G. Decelles, A. R. Carroll, and E. D. Goodman, Middle Tertiary contractile deformation, uplift, extension and rotation in the San Emigdio Range, southern California, *AAPG Bull., 74*, 665, 1990.

Hamilton, W., Mesozoic tectonics of southeastern California and southwestern Arizona (abstract), *Geol. Soc. Am. Abstr. Programs, 20*, 165, 1988.

Hauser, E. C. Potter, S. Burgess, J. Mutschler, R. Allmendinger, L. Brown, S. Kaufman, and J. Oliver, Crustal structure of the eastern Nevada from COCORP deep seismic reflection data, *Geol. Soc. Am. Bull., 99*, 833-844, 1987.

Haxel, G. B., R. M. Tosdal, and J. T. Dillon, Tectonic setting and lithology of the Winterhaven Formation: A new Mesozoic stratigraphic unit in southernmost California and southwestern Arizona, *U.S. Geol. Surv. Bull., 1599*, 19, 1985.

Hearn, T. M., and R. W. Clayton, Lateral velocity variations in southern California, I, Results for the upper crust from P_g waves, *Bull. Seismol. Soc. Am., 76*, 495-509, 1986a.

Hearn, T. M., and R. W. Clayton, Lateral velocity variations in southern California, II, Results for the lower crust from P_n waves, *Bull. Seismol. Soc. Am., 76*, 511-520, 1986b.

Henyey, T. L., D. Okaya, E. Frost, and T.V. McEvilly, CALCRUST (1985) seismic reflection survey, Whipple Mountains detachment terrane, California: An overview, *Geophys. J. R. Astron. Soc., 89*, 111-118, 1987.

Ingersoll, R. V., Tectonics of sedimentary basins, *Geol. Soc. Am. Bull., 100*, 1704-1719, 1988.

Jackson, J., and P. Molnar, Active faulting and block rotations in the western Transverse Ranges, California, *J. Geophys. Res., 95*, 22,073-22,089, 1990.

Jacobson, C. E., Structural geology of the Pelona Schist and Vincent Thrust, San Gabriel Mountains, California, *Geol. Soc. Am. Bull., 94*, 753-767, 1983.

Jacobson, C. E., The $^{40}Ar/^{39}Ar$ geochronology of the Pelona Schist and related rocks, southern California, *J. Geophys. Res., 95*, 509-649, 1990.

Jacobson, C. E., M. R. Dawson, and C. E. Postlethwaite, Structure, metamorphism, and tectonic significance of the Pelona, Orocopia, and Rand Schists, southern California, in *Metamorphism and Crustal Evolution of the Western United States*, Rubey Volume VII, edited by W. G. Ernst, pp. 976-997, Prentice-Hall, Englewood Cliffs, N. J., 1988.

Lawson, R., Seismic reflection data from the eastern Mojave Desert, M.S. thesis, Univ. of South. Calif., Los Angeles, 1989.

Leventhal, J. A., M. R. Reid, and A. Montana, A role for depleted mantle in Mesozoic plutonism of the eastern Mojave Desert? Evidence from xenoliths from Cima volcanic field, *Geol. Soc. Am. Abstr. Programs, 24*, 64, 1992.

Malin, P. E., M. H. Gillespie, P. C. Leary, and T. L. Henyey, Crustal structure near Palmdale, California, from borehole-determined ray parameters, *Bull. Seismol. Soc. Am., 71*, 1783-1803, 1981.

Malin, P. E., E. D. Goodman, T. L. Henyey, E. L. Ambos, D. A. Okaya, and T. L. McEvilly. The crustal evolution of the southern San Joaquin/Tejon embayment from CALCRUST seismic reflection and refraction profiling, paper presented at the Third International Workshop and Symposium on Seismic Probing of Continents and Their Margins, Australian National University, Canberra, Australia, 1988.

Mattinson, J. M., and E. W. James, Salinian block U/Pb age and isotopic variations: Implications for origin and emplacement of the Salinian terrane, in *Tectonostratigraphic Terranes of the Circum-Pacific Region, Earth Sci. Ser.*, vol.1, edited by D. G. Howell, pp. 215-226, Circum-Pacific Council for Energy and Mineral Resources, Houston, Tex., 1985.

May, D. J., Late Cretaceous intra-arc thrusting in southern California, *Tectonics, 8*, 1159-1173, 1989.

McWilliams, M., and Y. Li, Tectonic oroclinal bending of the southern Sierra Nevada batholith, *Science, 230*, 172-175, 1985.

Mereu, R. F., S. Mueller, and D. M. Fountain (Eds.), *Properties and Processes of Earth's Lower Crust, Geophys. Monogr. Ser.*, vol. 51, AGU, Washington, D. C., 1989.

Montana, A., M. Reid, and P. Holden, Subducted ocean-floor basalt beneath the Cima volcanic field, California, *Geol. Soc. Am. Abstr. Programs, 23*, 50, 1991.

Mukhopadhyay, B., W. I. Manton, and D. C. Presnall, Petrographic, chemical, and isotopic constraints on the origin of garnet pyroxenite xenoliths from the Big Creek volcanic pipe, Sierra Nevada Batholith, *Eos Trans. AGU, 69*, 1517, 1988.

Nourse, J. A., Geological evolution of two crustal scale shear zones, Ph.D. thesis, 392 pp., Calif. Inst. of Technol., Pasadena, 1989.

Nourse, J. A., and L. T. Silver, Structural and kinematic evolution of sheared rocks in the Rand thrust complex, northwest Mojave Desert (abstract), *Geol. Soc. Am. Abstr. Programs, 18*, 165, 1986.

Okaya, D. A., E. Karageorgi, T. V. McEvilly, and P. E. Malin, Removal of ground-induced vibroseis correlation artifacts by frequency-uncorrelated time filtering. paper presented at SEG Annual Meeting, Soc. of Explor. Geol., San Francisco, Calif., 1990.

Okaya, D. A., E. Karageorgi, T. V. McEvilly, and P. E. Malin, Removal of ground-induced vibroseis correlation artifacts by filtering in frequency-uncorrelated time space, *Geophysics, 57*, 916-926, 1992.

Pickett, D. A., and J. B. Saleeby, Thermobarometric constraints on the depth of exposure and conditions of plutonism and metamorphism at deep levels of the Sierra Nevada Batholith, Tehachapi Mountains, California, *J. Geophys, Res., 98*, 609-629, 1993.

Plescia, J. B., A gravity and magnetic study of the Tehachapi Mountains, California, Ph.D. thesis, Dep. of Geol., Univ. of South. Calif., Los Angeles, 1985.

Plescia, J. B., and G. J. Calderone, Paleomagnetic constraints on the timing of rotation of the Tehachapi Mountains, California, *Geol. Soc. Am. Abstr. Programs, 18*, 171, 1986.

Ross, D. C., Metagraywacke in the Salinian block, central Coast Ranges, California — And a possible correlative across the San Andreas fault, *U.S. Geol. Surv. J. Res. 4*, 683-696, 1976.

Ross, D. C., Mafic gneiss complex (batholithic root?) in the southernmost Sierra Nevada, CA, *Geology, 13*, 288-291, 1985.

Ross, D. C., The metamorphic and plutonic rocks of the southernmost Sierra Nevada, California, and their tectonic framework, *U.S. Geol. Survey Prof. Pap., 1381*, 159 pp., 1989.

Saleeby, J.B., Continent-Ocean transect, Corridor C2, Montery Bay offshore to the Colorado Plateau, GSA Map and Chart Series TRA C2, 2 sheets, scale 1:500,000, 87 pp., Geol. Soc. of Am., Boulder, Colo., 1986.

Saleeby, J. B., Progress in tectonic and petrogenic studies in an exposed cross-section of young (~100 Ma) continental crust, southern Sierra Nevada, California, in *Exposed Cross-sections of the Continental Crust*, edited by M. H. Salisbury and D. M. Fountain, pp. 137-158, Kluwer Academic, Norwell, Mass., 1990.

Saleeby, J. B., D. B. Sams, and R. W. Kistler, U/Pb zircon, strontium, and oxygen isotopic and geochronological study of the southernmost Sierra Nevada batholith, California, *J. Geophys. Res., 92*, 10,443-10,466, 1987.

Salisbury, M.H., and D.M. Fountain (Eds.), *Exposed Cross-sections of the Continental Crust*, Kluwer Academic, Norwell, Mass., 1990.

Sams, D. B., and J. B. Saleeby, Geology and petrotectonic significance of crystalline rocks of the southernmost Sierra Nevada, in *Metamorphism and Crustal Evolution of the Western United States*, Rubey Volume VII, edited by W. G. Ernst, pp. 865-893, Prentice-Hall, Englewood Cliffs, N. J., 1988.

Serpa, L., and R. Dokka, Reinterpretation of Mojave COCORP data: Implications for the structure of the Mojave Rift, *Geol. Soc. Am. Abstr. Programs, 20*, 230, 1988.

Sharry, J., The geology of the western Tehachapi mountains, California, Ph.D. thesis, 215 pp., Mass. Inst. of Technol., Cambridge, 1981.

Silver, L. T., Evidence and a model for west-directed early to Mid-Cenozoic basement overthrusting in southern California, *Geol. Soc. Am. Abstr. Programs, 14*, 617, 1982.

Silver, L. T., Paleogene overthrusting in the tectonic evolution of the Transverse Ranges, Mojave and Salinian regions, California, *Geol. Soc. Am. Abstr. Programs, 15*, 438, 1983.

Silver, L. T., and J. M. Mattinson, Orphan Salinia has a home, *Eos Trans. AGU, 67*, 1215, 1986.

Silver, L. T., and J. A. Nourse, The Rand Mountains Thrust complex in comparison with the Vincent Thrust-Pelona Schist relationship, southern California, *Geol. Soc. Am. Abstr. Programs, 18*, 185, 1986.

Silver, L. T., D. B. Sams, M. I. Bursik, R. W. Graymer, J. A. Nourse, M. A. Richards, and S. L. Salyards, Some observations on the tectonic history of the Rand Mountains, Mojave Desert, California, *Geol. Soc. Am. Abstr. Programs, 16*, 323, 1984.

Silver, L. T., H. P. Taylor Jr., and B. Chappell, Some petrological, geochemical and geochronological observations of the Peninsular Ranges batholith near the international border of the U.S.A. and Mexico, in *Mesozoic Crystalline Rocks: Peninsular Ranges Batholith and Pegmetites, Point Sal Ophiolite, Meeting Guidebook*, edited by P. L. Abbott and V. R. Todd, pp. 83-110, Geological Society of America, Boulder, Colo., 1979.

Wernicke, B. The fluid crustal layer and its implications for continental dynamics, in *Exposed Cross-sections of the Continental Crust*, edited by M. H. Salisbury and D. M. Fountain, pp. 509-544, Kluwer Academic, Norwell, Mass., 1990.

Wernicke, B. P., and G. J. Axen, On the role of isostacy in the evolution of normal fault systems, *Geology, 16*, 848-851, 1988.

Wernicke, B., and B. C. Burchfiel, Modes of extension tectonics, *J. Struct. Geol., 4*, 105-115, 1982.

Wiese, J. H., Geology and mineral resources of the Neenach quadrangle, California, *Calif. Dept. Nat. Res. Div. Mines Bull., 153* , 53 pp., 1950.

Yilmaz, O., *Seismic Data Processing*, Society of Exploration Geophysicists, Tulsa, Okla., 1987.

E. D. Goodman, Exxon Production Research Co., Box 2189, Houston, TX 77252-2189.

T. L. Henyey, Y. G. Li, and D. A. Okaya, Department of Geological Sciences, University of Southern California, Los Angeles, CA 90089. (email: henyey; ygli; okaya; @coda.usc.edu)

P. E. Malin, Department of Geology, Box 90235, Duke University, Durham, NC 27708-0235. (email: pem@vaino.geo.duke.edu)

J. B. Saleeby, Division of Geological And Planetary Sciences, California Institute of Technology, Pasadena, CA 91125.

(Received May 10, 1993; Revised August 3, 1994;
accepted August 11, 1994.)